tion of SPARC in situ. As shown in Figure 4A, a higher level of SPARC-associated Cy-3 fluorescence was observed in the subepithelial regions of the limbus compared with the central cornea. The difference can be appreciated when compared with the uniform fluorescence observed in the overlying epithelial cells (Figure 4B). Thus, SPARC is constitutively expressed in the limbal stroma by resident fibroblasts without the stimulation of a wound healing process.

Cell adhesion assay: In order to observe the effects of SPARC on corneal epithelial cells in vitro, an immortalized cell line (HCEC) were used to observe for changes in cell adhesion and morphology. The addition of SPARC in the culture supernatant resulted in rounding of individual HCEC after 3 h (Figure 5). The difference was statistically significant using a rounding index originally described by Lane and Sage [16] (n=5).

DISCUSSION

SPARC is a 43 kDa protein that contains a COOH-terminal EC module with two Ca^{2+}-binding domains, a follistatinlike module, and an NH_2-terminal acidic module [7]. The expression of SPARC by corneal stromal cells has been reported to play a role in the wound healing response, evidenced by the upregulation of SPARC by the fibroblast and myofibroblast phenotype [9]. However, SPARC was not detected in quiescent corneal stromal cells, and hence, the major function of the protein was speculated to be related to wound healing. Conversely, SPARC secreted by epithelial cells was shown to induce contraction of stromal fibroblasts in vitro, suggesting that SPARC is a key protein in epithelial/stromal interaction of the cornea [17]. SPARC has also been proposed to be involved in corneal epithelial migration and stratification following mechanical ablation [8].

We found that limbal fibroblasts secreted higher levels of SPARC compared to central corneal fibroblasts in vitro without stimulation by serum or cytokines, and also in vivo without any wound-healing stimuli. SPARC was one of only a few proteins detectable by proteomic analysis in the limbal fibroblast supernatant, suggesting a functional role in the homeostasis of the limbal structure. Although it can be argued that corneal fibroblasts cultured in vitro are not the same as keratocytes in vivo, experiments requiring large quantities of cells would not be possible without in vitro expansion. All cells used in the current study were first expanded in vitro using serum containing 10% serum, therefore, the phenotype of these cells at the time of analysis is not necessarily consistent with the normal phenotype. The results of preotomics alone, therefore, have limits without further analysis. Inter-

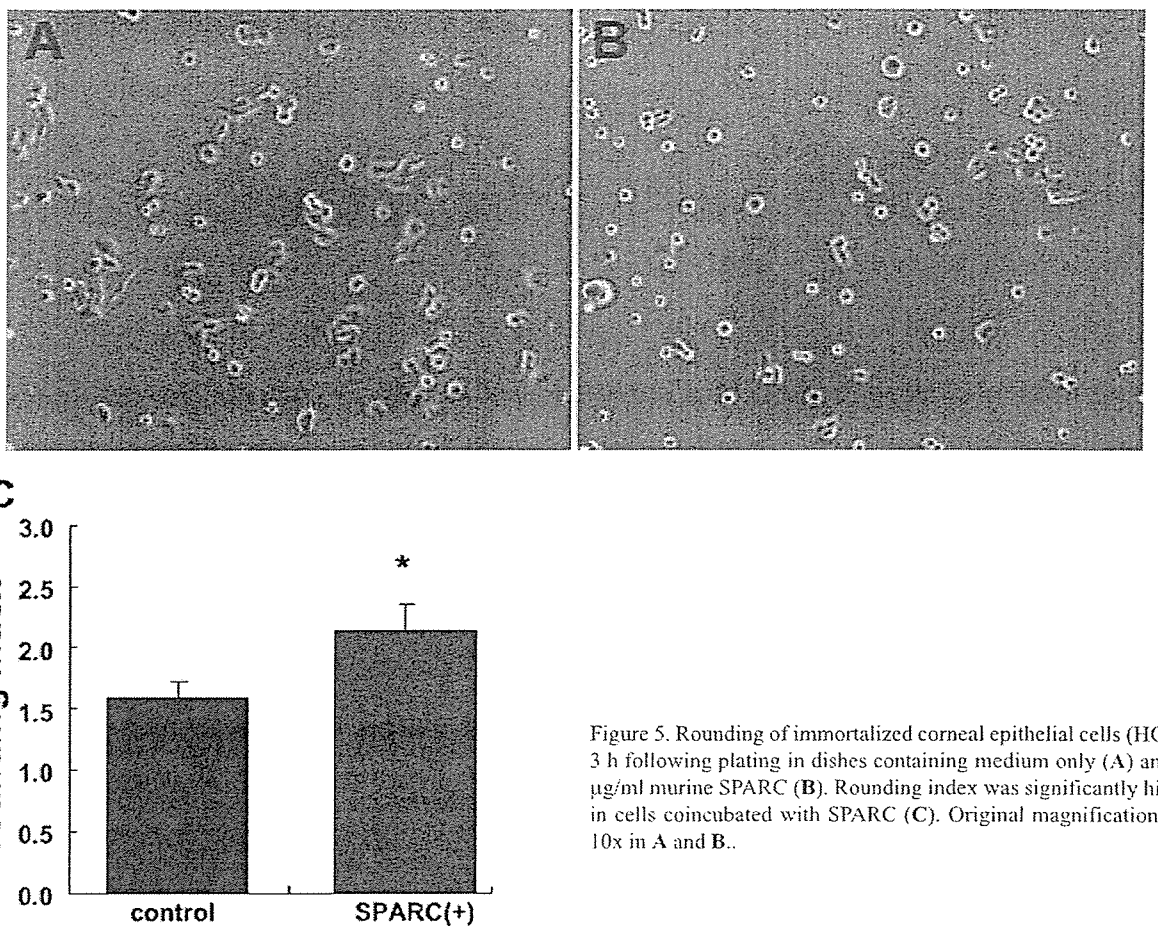

Figure 5. Rounding of immortalized corneal epithelial cells (HCEC) 3 h following plating in dishes containing medium only (**A**) and 10 µg/ml murine SPARC (**B**). Rounding index was significantly higher in cells coincubated with SPARC (**C**). Original magnification was 10x in A and B..

estingly, one of the proteins detected in the limbal cell supernatant was vimentin, an intracellular intermediate fiber, suggesting that some of the proteins in the supernatant may have been the result of apoptosis. We did not pursue this issue further, and chose to focus on SPARC which is a secreted protien.

Figure 4 shows the immunohistochemistry of SPARC in donor cornea tissue. The result shows that SPARC is expressed more in the limbal stroma, reflecting the results of real time RT-PCR and western blots of cell supernatants. We have also found through immunohistochemistry that epithelial cells were positive for SPARC, while western blots only detected trace levels of SPARC from cell lysates and supernatant of primary cultured epithelial cells. This may be explained by the fact that SPARC is secreted by corneal epithelial cells during wound repair [8,17], and that primary cells in vitro may be in a state similar to epithelial cells undergoing wound healing.

We focused on the function of SPARC, since the matricellular protein has been reported to regulate the adhesion of bovine aortic endothelial cells [10]. Using a previously described adhesion assay, we found that exogenous SPARC inhibited adhesion of a human corneal epithelial cell line, which may be due to the Ca^{2+}-binding ability of SPARC. Espana et al. [6] have previously reported that limbal stroma, and not corneal stroma, was required to maintain an undifferentiated phenotype (K3 negative, Cx 43-low) in corneal epithelial cell sheets. This implies that soluble factors expressed by limbal fibroblasts may be involved in this phenomenon. The extracellular matrix and basement membrane components of the limbal area are distinct from the central cornea, as reported by several studies [18,19]. SPARC is also involved in the migration and invasion of prostate cancer cells [11] and breast cancer cells [20] through the activation of matrix metalloproteinase 2 (MMP2). These are several properties that are expected of matricellular proteins in the putative limbal stem cell niche. Interestingly, the MMP2-specific inhibitor, TIMP2 was also preferentially detected in the supernatant of limbal fibroblasts, suggesting that an intricate network based on a balance of effectors and inhibitors may be involved in the homeostasis of the limbal stem cell niche.

Growth factors such as keratinocyte growth factor and hepatocyte growth factor are also mediators of fibroblast/epithelial interaction involved in epithelial proliferation and migration [21]. Although the network of epithelial/mesenchymal interaction in the corneal limbus is sure to involve a wide variety of matricellular proteins, cytokines, and growth factors, the inhibition of cellular adhesion and cell/cell interaction by SPARC may be a major component of the limbal microenvironment. We found that the human amniotic membrane (AM) also contains SPARC (data not shown), which may partially explain the ability of AM to preserve the undifferentiated state of limbal epithelial cell in vitro [22]. While further studies are required to elucidate the interactions of soluble factors involved in the limbal niche, a combination of such components may be used to enrich limbal stem cells in vitro.

ACKNOWLEDGEMENTS

This study was partly supported by a grant of Advanced and Innovational Research Program in Life Sciences from the Ministry of Education, Culture, Sports, Science and Technology of Japan.

REFERENCES

1. Chen Z, de Paiva CS, Luo L, Kretzer FL, Pflugfelder SC, Li DQ. Characterization of putative stem cell phenotype in human limbal epithelia. Stem Cells 2004; 22:355-66.
2. Kenyon KR, Tseng SC. Limbal autograft transplantation for ocular surface disorders. Ophthalmology 1989; 96:709-22; discussion722-3.
3. Tsubota K, Satake Y, Kaido M, Shinozaki N, Shimmura S, Bissen-Miyajima H, Shimazaki J. Treatment of severe ocular-surface disorders with corneal epithelial stem-cell transplantation. N Engl J Med 1999; 340:1697-703.
4. Koizumi N, Inatomi T, Suzuki T, Sotozono C, Kinoshita S. Cultivated corneal epithelial transplantation for ocular surface reconstruction in acute phase of Stevens-Johnson syndrome. Arch Ophthalmol 2001; 119:298-300.
5. Pellegrini G, Traverso CE, Franzi AT, Zingirian M, Cancedda R, De Luca M. Long-term restoration of damaged corneal surfaces with autologous cultivated corneal epithelium. Lancet 1997; 349:990-3.
6. Espana EM, Kawakita T, Romano A, Di Pascuale M, Smiddy R, Liu CY, Tseng SC. Stromal niche controls the plasticity of limbal and corneal epithelial differentiation in a rabbit model of recombined tissue. Invest Ophthalmol Vis Sci 2003; 44:5130-5.
7. Brekken RA, Sage EH. SPARC, a matricellular protein: at the crossroads of cell-matrix communication. Matrix Biol 2001; 19:816-27.
8. Latvala T, Puolakkainen P, Vesaluoma M, Tervo T. Distribution of SPARC protein (osteonectin) in normal and wounded feline cornea. Exp Eye Res 1996; 63:579-84.
9. Berryhill BL, Kane B, Stramer BM, Fini ME, Hassell JR. Increased SPARC accumulation during corneal repair. Exp Eye Res 2003; 77:85-92. Erratum in: Exp Eye Res 2003; 77:643.
10. Sweetwyne MT, Brekken RA, Workman G, Bradshaw AD, Carbon J, Siadak AW, Murri C, Sage EH. Functional analysis of the matricellular protein SPARC with novel monoclonal antibodies. J Histochem Cytochem 2004; 52:723-33.
11. Jacob K, Webber M, Benayahu D, Kleinman HK. Osteonectin promotes prostate cancer cell migration and invasion: a possible mechanism for metastasis to bone. Cancer Res 1999; 59:4453-7.
12. Araki-Sasaki K, Ohashi Y, Sasabe T, Hayashi K, Watanabe H, Tano Y, Handa H. An SV40-immortalized human corneal epithelial cell line and its characterization. Invest Ophthalmol Vis Sci 1995; 36:614-21.
13. Kajiwara H, Kaneko T, Ishizaka M, Tajima S, Kouchi H. Protein profile of symbiotic bacteria Mesorhizobium loti MAFF303099 in mid-growth phase. Biosci Biotechnol Biochem 2003; 67:2668-73.
14. Perkins DN, Pappin DJ, Creasy DM, Cottrell JS. Probability-based protein identification by searching sequence databases using mass spectrometry data. Electrophoresis 1999; 20:3551-67.
15. Girard JP, Springer TA. Modulation of endothelial cell adhesion by hevin, an acidic protein associated with high endothelial venules. J Biol Chem 1996; 271:4511-7.

16. Lane TF, Sage EH. Functional mapping of SPARC: peptides from two distinct Ca+(+)-binding sites modulate cell shape. J Cell Biol 1990; 111:3065-76.
17. Mishima H, Hibino T, Hara H, Murakami J, Otori T. SPARC from corneal epithelial cells modulates collagen contraction by keratocytes. Invest Ophthalmol Vis Sci 1998; 39:2547-53.
18. Ljubimov AV, Burgeson RE, Butkowski RJ, Michael AF, Sun TT, Kenney MC. Human corneal basement membrane heterogeneity: topographical differences in the expression of type IV collagen and laminin isoforms. Lab Invest 1995; 72:461-73.
19. Fukuda K, Chikama T, Nakamura M, Nishida T. Differential distribution of subchains of the basement membrane components type IV collagen and laminin among the amniotic membrane, cornea, and conjunctiva. Cornea 1999; 18:73-9.
20. Gilles C, Bassuk JA, Pulyaeva H, Sage EH, Foidart JM, Thompson EW. SPARC/osteonectin induces matrix metalloproteinase 2 activation in human breast cancer cell lines. Cancer Res 1998; 58:5529-36.
21. Li DQ, Tseng SC. Three patterns of cytokine expression potentially involved in epithelial-fibroblast interactions of human ocular surface. J Cell Physiol 1995; 163:61-79.
22. Grueterich M, Espana EM, Tseng SC. Ex vivo expansion of limbal epithelial stem cells: amniotic membrane serving as a stem cell niche. Surv Ophthalmol 2003; 48:631-46.

The print version of this article was created on 11 May 2006. This reflects all typographical corrections and errata to the article through that date. Details of any changes may be found in the online version of the article.

Ocular Surface Epithelial Cells Up-Regulate HLA-G When Expanded In Vitro on Amniotic Membrane Substrates

Kazunari Higa, PhD, Shigeto Shimmura, MD,† Jun Shimazaki, MD,† and Kazuo Tsubota, MD*‡*

Purpose: To study the modulation of immunoregulatory genes in ocular surface epithelial cells cultured on amniotic membrane (AM).

Methods: Microarray analysis was performed in a conjunctival epithelial cell line (CCL20.2) expanded on denuded AM. Among the genes that were upregulated by an AM substrate compared with collagen-coated dishes, the fetal nonclassic major histocompatibility complex molecule, HLA-G, was found to be the only immunoregulatory gene up-regulated by more than 2.5-fold. Because CCL20.2 is contaminated by HeLa cells, expression of HLA-G mRNA was confirmed in primary-cultured limbal (LE) and conjunctival epithelial (CE) cells by reverse transcriptase-polymerase chain reaction (RT-PCR), semiquantitative real-time PCR, immunocytochemistry, and Western blot analysis. A functional assay was performed using an HLA-G–transfected K-562 human erythroleukemia cell line.

Results: Freshly dissociated limbal epithelial cells express HLA-G mRNA; however, protein levels were low. Western blots and immunocytochemistry showed that both LE and CE cells upregulated the HLA-G protein when cultured on collagen-coated dishes and on AM. HLA-G mRNA levels were significantly higher in CE cultured on AM compared with collagen. Natural killer (NK) cell–induced cell lysis of an HLA class I–negative K-562 human erythroleukemia cell line was slightly reduced when transfected with LE-derived HLA-G mRNA.

Conclusion: CE and LE cells express functional HLA-G when expanded ex vivo, which may affect inflammation and immune reaction when transplanted to the ocular surface.

Key Words: HLA-G, amniotic membrane, corneal epithelium, conjunctival epithelium, cornea immune responses

(*Cornea* 2006;25:715–721)

Numerous investigators have reported the use of amniotic membrane (AM) in ocular surface reconstruction since Kim and Tseng[1] reinstated the technique in the modern era. AM is used mainly as either a graft, intended to function as a substrate for overlying epithelium, or as a patch to temporarily cover the ocular surface while the host tissue undergoes wound healing. The use of AM was integral in our experience with allograft limbal transplantation (ALT) for reconstructing the ocular surface in severe cicatricial disease.[2–4] AM is also used as a carrier for transplanting ex vivo cultured sheets of corneal epithelium[5] and oral mucosa epithelium.[6]

The effects of AM on the ocular surface were initially perceived as somewhat of a "black box," with many undefined characteristics of both soluble and nonsoluble components of AM cells and stroma. The anti-inflammatory actions of AM have been associated with the production of various cytokines,[7] regulation of growth factor expression,[8,9] and the release of proteinase inhibitors.[10] Direct interaction of AM with invading inflammatory cells may be involved in the elimination of leukocytes from the ocular surface.[11,12] Another important aspect of using AM on the ocular surface is its antiangiogenic property,[13–15] which is vital in maintaining a transparent ocular surface, and may work in suppressing immunologic rejection of allogenic cells and tissue.

To further explain the effects of AM, we hypothesized that AM may have direct immune-regulatory functions on surrounding cells when transplanted to the ocular surface. It is well documented that placental tissue, including AM, suppresses the semi-allo-immune response of the mother against the fetus.[16,17] Ueta et al[18] indicated that human AM is capable of inhibiting alloreactive T-cell response including cell division, proliferation, and T_H1/T_H2 cytokine synthesis in vitro. On the basis of these findings, we sought to study the expression and function of HLA-G, an immunoregulatory protein found to be upregulated in an initial screening by microarray analysis of cells cultured on AM.

MATERIALS AND METHODS

Cell Culture

The JAR (HLA-G$^-$) choriocarcinoma cell line, the JEG-3 (HLA-G$^+$) choriocarcinoma cell line, and the CCL20.2 conjunctival cell line were purchased from ATCC (American Type Culture Collection, Rockville, MD). Denuded AM was prepared as previously described.[19] Preserved AMs were rinsed in phosphate-buffered saline (PBS; 3 times), spread onto culture dishes, frozen at −80°C, and air-dried at room temperature. AM-coated dishes were stored at −80°C until use. Corneoscleral tissue from human donor eyes was obtained from Northwest Lions Eye Bank, and limbal rims were

Received for publication April 13, 2005; accepted November 23, 2005.
From the *Cornea Center, Tokyo Dental College, Chiba, Japan; the †Department of Ophthalmology, Tokyo Dental College, Chiba, Japan; and the ‡Department of Ophthalmology, Keio University School of Medicine, Tokyo, Japan.
Supported by a grant from the Japan Health Sciences Foundation and by a grant of the Ministry of Health and Walfare (Saisei, H15-13).
Reprints: Shigeto Shimmura, MD, Cornea Center, Ichikawa General Hospital, Tokyo Dental College, 5-11-13 Sugano, Ichikawa, Chiba 272-8513 Japan (e-mail: shimmura@tdc.ac.jp).

preserved for experiments after the central corneal button was used for corneal transplantation. After careful removal of excess sclera, iris, and corneal endothelium, limbal segments were placed in either collagen-coated dishes (Iwaki: Asahi Technoglass, Funabashi, Japan) or on AM-coated dishes. Limbal explants were cultured for 2 weeks at 37°C, 5% CO_2 in supplemented hormonal epithelial medium (SHEM), made of an equal volume of HEPES-buffered Dulbecco's modified Eagle's medium (DMEM) and Ham's F12 (Invitrogen, Carlsbad, CA) containing bicarbonate, 0.5% dimethylsulfoxide (Sigma, St. Louis, MO), 10 ng/mL human epidermal growth factor (EGF: Invitrogen), 5 μg/mL insulin (Sigma), 100 ng/mL cholera toxin (Invitrogen), 15% fetal bovine serum (FBS), 70 μg/mL penicillin (Wako Pure Chemical Industries, Osaka, Japan), and 140 ng/mL streptomycin (Wako). Expanded cells were cultured serum-free for 3 days in Epilife containing HCGS (Kurabo Co., Osaka, Japan) at 37°C, 5% CO_2.

Microarray Analysis

The Atlas Glass Total RNA Isolation Kit (BD, Franklin Lakes, NJ) was used to isolate total RNA from CCL20.2 cells cultivated on either collagen or AM-coated dishes. After RNA was isolated, genomic DNA was removed using DNAse (Qiagen, Hilden, Germany). The targets were prepared using the Atlas Glass Fluorescent Labeling Kit (Clontech Laboratories). Aminoallyl-dUTP was incorporated during first-strand cDNA synthesis. Fluorescent dye (Cy3 or Cy5) was covalently coupled to aminoallyl-dUTP in the first-strand cDNA. Absorbance of each target was determined by optical density measurements at 260 nm (DNA) and either 550 (Cy3) or 650 nm (Cy5). The total dye content (pmoles), amount of probe (nanograms), and specific activity (number of Cy molecules incorporated per number of bases) was calculated for each target synthesized. Once the target quality was determined to be appropriate, targets were hybridized to probes immobilized on glass slides. The slides were hybridized overnight at 50°C using the GlassHyb Hybridization Solution (BD). After we quantified gene expression with Atlas Glass Microarrays, analysis and visualization of data were done by the Atlas Navigator software (BD). The fluorescence intensity of each spot was calculated using the histogram quantitation method, which has the major advantage of being simple and stable.

Reverse Transcriptase-Polymerase Chain Reaction and Real-Time Polymerase Chain Reaction

Total RNA was isolated from cells using the SV total RNA isolation system (Promega, Madison, WI) according to the manufacturer's recommendations and verified by electrophoresis in denaturing 1.0% agarose gel. cDNA was prepared from total RNA with oligo(dT) priming and AVM reverse transcriptase (RT) XL (Takara, Bio, Ptsu, Shiga, Japan) by incubation of a 25-μL mixture at 41°C for 1 hour. The cDNA was subjected to polymerase chain reaction (PCR) by using the following HLA-G–specific oligonucleotide primers: forward primer 5′-cgcggaccaaccctcttcctgctactctcgg-3′ and reverse primer 5′-cggggtaccgcctcgctctggttggtagtagcc-3′. PCR amplifications (1 μL of cDNA in a total reaction volume of 50 μL) were run at 98°C for 10 seconds, at 56°C for 20 seconds, and at 72°C for 30 seconds (30 cycles). The amplification of β-actin was performed in the same manner to check cDNA quality. JAR cells were used as negative control, and JEG-3 cells were used as positive control. PCR amplification products were separated by electrophoresis on a 2% agarose gel.

Real-time RT-PCR was used to semiquantify HLA-G expression in primary cultured limbal and conjunctival epithelium. The method allows for the direct detection of PCR products during the exponential phase of the reaction, combining amplification and detection using TaqMan chemistry (Applied Biosystems, Foster City, CA) and the ABI Prism 7700 Sequence Detection System (Applied Biosystems). The TaqMan probe was designed to anneal to the target sequence, HLA-G α−1 domain, between the classic forward and reverse primers.

Immunocytochemistry

Cytospin preparations of limbal epithelial cells (5.0×10^4 cells/slide) were prepared by Auto Smear CF-12D (Sakura Finetechnical, Tokyo, Japan). Samples were fixed in cold acetone for 10 minutes and washed with PBS. Cytospin preparations were blocked with 10% normal donkey serum (Chemicon International, Temecula, CA) for 1 hour. Sections were incubated for 60 minutes at room temperature with a monoclonal antibody (MEM-G/9, 1/100 dilution; Abcam, Cambridge, UK) that reacts with the native form of human HLA-G on the cell surface, as well as with soluble HLA-G molecules. Isotype normal mouse immunglobulin G1 (IgG1) (Dako Cytomation, Glostrup, Denmark) was used as control. After washing with TBST (0.825 mmol/L Tris, 136.9 mmol/L NaCl, 1.34 mmol/L KCl, 0.1% Tween 20; Sigma), the section was reacted with rhodamine-conjugated donkey anti–mouse IgG secondary antibody (Jackson Immuno Research, West Grove, PA) for 30 minutes at room temperature. After 3 washes with TBST, the sections were incubated with 1 μg/mL 4′,6-diamidino-2-phenylindole (DAPI; Dojindo Laboratories, Tokyo, Japan) at room temperature for 5 minutes. Finally, sections were washed 3 times in TBST, and a coverslip was fixed using an antifading mounting medium (50 mmol/L Tris buffer saline, 90% glycerin [Wako], 10% 1,4-diazabicyclo (2,2,2) octane [Wako]).

Western Blot Analysis

Samples were dissolved with lysis buffer (50 mmol/L Tris-HCl, pH 7.4, 150 mmol/L NaCl, 1% Nonidet P-40; Calbiochem, Darmstadt, Germany) and homogenated. Samples were incubated for 40 minutes at 4°C and centrifuged at 15,000 rpm for 30 minutes at 4°C. Protein concentration of the supernatant was determined by the DC protein assay (Bio-Rad Laboratory, Hercules, CA). All samples were diluted in 2× sample buffer (100 mmol/L Tris-HCl [pH 6.8], 4% sodium dodecyl sulfate [Invitrogen], 20% glycerol [Wako], 12% 2-mercaptoethanol [Wako]) and boiled. Twenty micrograms of each sample was loaded on a Novex NuPAGE 10% Bis-Tris gel (Invitrogen) and transferred onto polyvinylidene difluoride (PVDF) membranes (Millipore, Billerica, MA). Membranes were blocked with 5% skim milk (Difco Laboratories, Detroit, MI), 1.5% normal goat serum, and PBS for 60 minutes at room

temperature. Membranes were reacted with an anti–HLA-G (MEM-G1) antibody (Serotec, Oxford, UK) for 60 minutes at room temperature. After 3 washes in TBST, donkey biotinylated anti–mouse IgG (Jackson ImmunoResearch) was added for 30 minutes at room temperature. Protein bands were visualized by the Vectastain ABC Elite Kit (Vector Laboratories, Bulingame, CA) and DAB (Vector Laboratories) as substrate.

Transfectants

The K-562 human erythroleukemia cell line (ATCC) was maintained in IMDM (Invitrogen) supplemented with 100 IU/mL penicillin (Wako)/100 μg/mL streptomycin (Wako) and FCS (Sanko Zyunyaku Co. Ltd., Tokyo, Japan). After successful amplification of the full-length human *HLA-G* gene from corneal epithelium, HLA-G plasmids were generated by cloning HLA-G cDNA into a green fluorescent protein (GFP) construct (phrGFP1-Puromycin; Stratagene, La Jolla, CA). GFP vector transfectants (phrGFP1-Puromycin) were used as control. Transfection was done using the Effectene Transfection Reagent (Qiagen) and the Nucleofector electroporation device (Amaxa, Cologne, Germany). Cells were selected in media containing 100 μg/mL Puromycin (Sigma).

Peripheral Blood Mononuclear Cells and Purified Natural Killer Cells

Peripheral blood mononuclear cells (PBMCs) were isolated from normal healthy volunteers by density gradient centrifugation using Ficoll-Paque PLUS (Amersham Biosciences, Uppsala, Sweden). $CD56^+$ natural killer (NK) cells were purified using the NK cell isolation kit II (Miltenyi Biotec, Bergisch Gladbach, Germany). Purity of the isolated populations used in the experiments was greater than 97% $CD3^-CD56^+$.

Cytotoxic Assay

The cytolytic action of NK cells against K-562 HLA-G transfectants was measured by bromodeoxyuridine (BrdU) release using the Cellular DNA Fragmentation enzyme-linked immunosorbent assay kit (Roche, Mannheim, Germany), in which effector cells (NK cells) were mixed with 1×10^5 BrdU-labeled target cells (K-562 transfectants) at the same effector:target ratio. After a 24-hour incubation at 37°C in a humidified 5% CO_2 incubator, DNA fragments by cell-mediated cytotoxicity were measured in the supernatant using a BrdU-specific monoclonal antibody. The percentage of cell lysis was calculated as follows: Percent specific lysis = $[(OD_{450}$ experimental well − OD_{450} spontaneous release)/(OD_{450} maximum release − OD_{450} spontaneous release)] × 100.

RESULTS

Microarray Analysis

To screen for changes in gene expression by ocular surface epithelial cells under different culture conditions, CCL20.2 cells were cultured on either collagen- or AM-coated dishes and compared by microarray. Table 1 shows a list of genes that were upregulated by an AM substrate. There was a 2.6-fold increase in HLA-G expression, which was the only gene with a known immunoregulatory function. Because ATCC warns of a possible contamination of CCL20.2 cells by HeLa cells, we further studied the expression of HLA-G in freshly dissociated limbal epithelial cells, as well as primary cultures of limbal and conjunctival epithelial cells.

Cultured Conjunctival and Limbal Epithelial Cells Express HLA-G mRNA

HLA-G mRNA was expressed by primary conjunctival and limbal epithelial cells when cultured on collagen, as well as AM (Fig. 1). Freshly dissociated limbal epithelial cells also expressed HLA-G by RT-PCR. JAR cells (HLA-G negative) and K562 cells (HLA class I negative) were used as a negative control and JEG-3 cells were used as a positive control. No mRNA was detected from AM samples without seeded cells (data not shown), ruling out the possibility of contamination by AM mRNA.

Real-time PCR was used to semiquantitate HLA-G expression by each cell type when cultured on AM. In accordance with microarray results, CCL20.2 showed a 2.0-fold increase ($P < 0.05$) in HLA-G expression when cultured on AM (Fig. 2A). Similarly, primary conjunctival epithelial cells underwent a 1.9-fold increase ($P < 0.05$). Primary cultured limbal epithelial cells also had a tendency for upregulating HLA-G, but the difference was not statistically significant compared with collagen (Fig. 2A).

HLA-G Protein Expression by Limbal Epithelial Cells

Immunocytochemistry was done on cytospin samples of cultured primary limbal cells, JAR cells, and JEG-3 cells. Conjunctival cells were not available because of the scarcity of surgically removed tissue. Although freshly dissociated limbal cells did not express appreciable levels of HLA-G on the cell surface (Fig. 3A), primary limbal epithelial cells cultured on AM showed clusters of positive-staining cells (Fig. 3B). The specificity of HLA-G staining was confirmed by negative (JAR) and positive (JEG-3) controls (Fig. 3C and D). HLA-G protein was also compared by Western blot (Fig. 4). Similar to immunocytochemistry, HLA-G was detected in cultured limbal epithelial cells, but not by freshly dissociated cells from limbal tissue.

Inhibition of Cell Lysis by HLA-G–Transfected K-562 Cells

To show the immunosuppressive function of the HLA-G molecule, we transfected the *HLA-G* gene derived from limbal epithelium into the HLA class 1–negative K-562 cell by using a GFP vector. HLA-G was successfully transfected into K-562 as shown by RT-PCR (Fig. 5A). When activated NK cells isolated from fresh peripheral blood were cocultured with transfected K-562, cell lysis detected by BrdU release was slightly lower in HLA-G–transfected cells than in control (Fig. 5B).

DISCUSSION

The absence of a harmful maternal immune response against the semiallogenic fetus has long been a major enigma in current biology. During mammalian pregnancy, fetal cells invade the uterine structures and survive without immunologic rejection.[20] It has now become evident that trophoblast cells

TABLE 1. Alteration of Genes in Microarray Analysis

GenBank #	Gene	Ratio (AM/dish)
NM_005876	Nuclear protein, marker for differentiated aortic smooth muscle and downregulated with vascular injury	2.5
NM_001174	Rho GIPase activating protein 6	2.9
NM_000156	Guadinoacetate *N*-methyltransferase	2.6
NM_000407	Glycoprotein 1b [platelet], β-polypeptide	3.8
NM_000733	CD3E antigen, epsilon polypeptide [TiT3 complex]	3.0
NM_000741	Cholinergic receptor, muscarinic 4	3.5
NM_004357	CD 151 antigen	2.7
NM_003822	Nuclear receptor subfamily 5, group A, member 2	2.7
NM_004456	Enhancer of zeste (*Drosophila*) homolog 2	3.3
NM_001731	B-cell translocation gene 1, antiproliferative	3.9
NM_001615	Actin, gamma 2, smooth muscle, enteric	3.2
NM_001567	Inositol polyphosphate phosphatase-like 1	0.4
NM_002282	Keratin, hair, basic, 3	2.8
NM_005576	Lysyl oxidase-like 1	0.2
NM_002127	HLA-G histocompatibility antigen, class I, G	2.6
NM_000290	Phosphoglycerate mulase 2 [muscle]	2.9
NM_002499	Neogenin (chicken) homolog 1	3.0
NM_002571	Progestagen-associated endometrial protein (placental protein 14, pregnancy-associated endometrial α-2-globulin, α uterine protein)	3.5
NM_002722	Pancreatic polypeptide	4.9
NM_002824	Parathymosin	2.7
NM_002846	Protein tyrosine phophatase, receptor type, N	2.8
NM_005394	Postmeiotic segregation increased 2-like 8	2.5
NM_001051	Somatostatin receptor 3	4.7
NM_002911	Regulator of nonsense transcripts 1	4.0
NM_003006	Selectin P ligand	4.9
NM_003178	Synapsin II	2.5
NM_003281	Troponin I, skeletal, slow	3.6
NM_006945	Small proline-rich protein 2B	3.4
NM_003611	Chromosome X open reading frame 5	3.7

express the nonclassical class I HLA molecules HLA-G[21,22] and HLA-E[23] and the classic class I HLA molecule HLA-C, which is expressed mainly during the first trimester.[24,25] The role of HLA-G in the fetal membrane is to protect cytotrophoblasts against NK cytolysis by maternal NK cells.[26] Indeed, the expression of HLA-G on the cell surface of various cells protected susceptible target cells from NK-mediated cytotoxicity.[27–31]

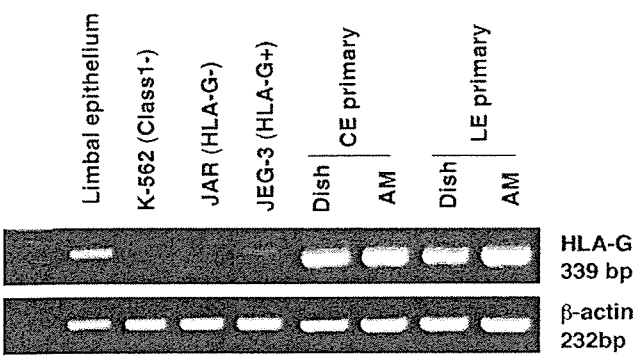

FIGURE 1. RT-PCR of HLA-G mRNA from primary LE and CE cultures (P0) on collagen and AM. JAR and K562 cells (HLA class 1 negative) were loaded as negative control and JEG-3 was loaded as positive control. Freshly dissociated limbal epithelium also expressed HLA-G mRNA.

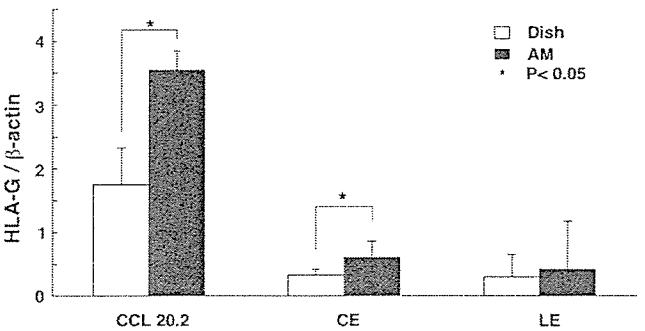

FIGURE 2. Semiquantitative real-time RT-PCR of HLA-G in CCL20.2, primary LE, and CE cells. HLA-G expression increased significantly in CCL20.2 and CE when cultured on AM instead of collagen. Although a similar trend was observed in LE, the increase was not statistically significant. Mean ± SD (n = 5). $^*P < 0.05$.

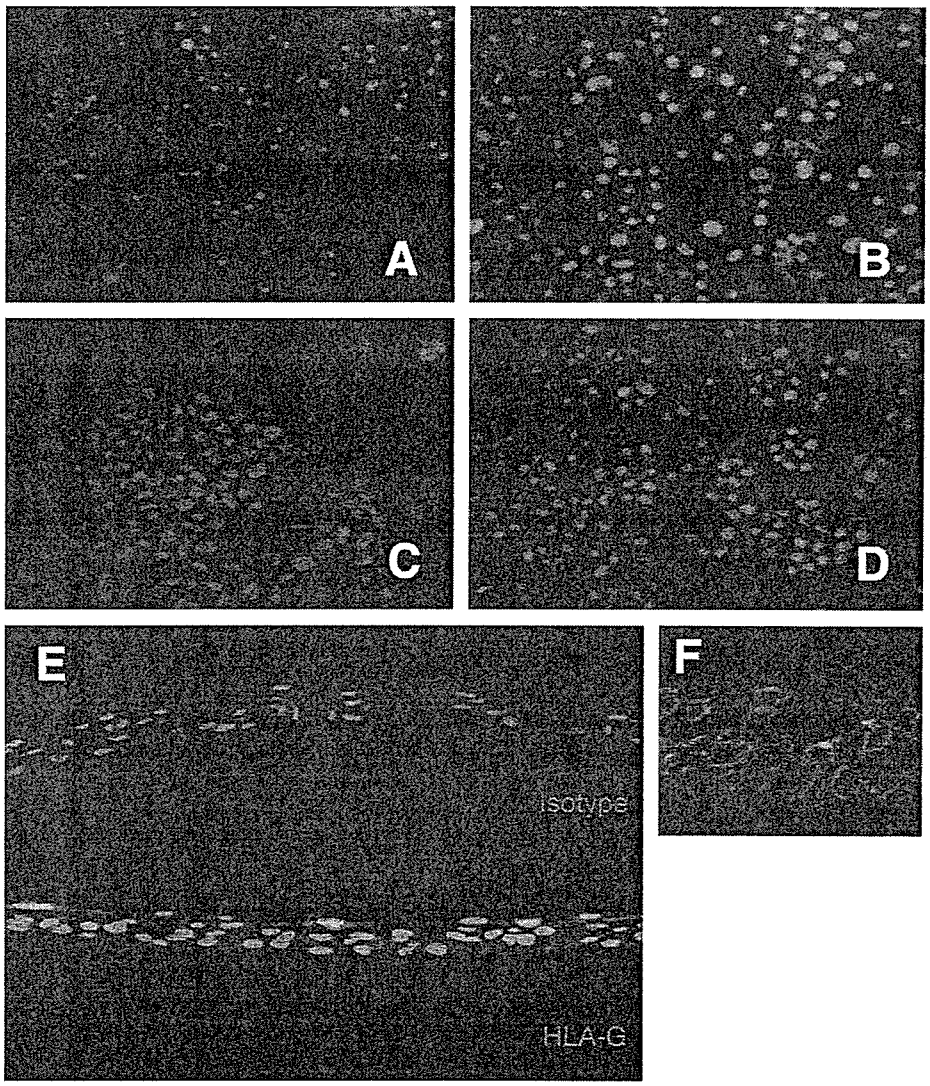

FIGURE 3. Immunocytochemistry of HLA-G in cytospin samples of freshly dissociated limbal epithelium (A) and primary cultures (P0) of LE cells explanted on AM (B). JAR, HLA-G–negative control (C); JEG-3, HLA-G–positive control (D). E, Immunocytochemistry in primary cultured limbal epithelial cells. (F), Positive control using placental tissue. Original magnification, ×200.

HLA-G can be expressed by adult tissue in the presence of inflammation or when cells are cultivated in vitro where the expression of HLA-G is selectively upregulated by cytokines such as interferon-γ[32] and interleukin-10.[33] One such example was reported by Wiendl et al,[34] who recently showed that muscle fibers in inflammatory myopathies and cultured myoblasts express the HLA-G molecule. In this report, we showed the upregulation of HLA-G in cultivated conjunctival and corneal cells. It is interesting that only HLA-G mRNA was upregulated when an AM substrate was used, whereas other class 1 HLA molecules, namely HLA-C and HLA-E, slightly decreased on microarray analysis (data not shown). We used the CCL20.2 conjunctival cell line for microarrays because a large number of cells was required as a source of RNA, which was not possible with primary cultured cells. Because CCL20.2 cells are contaminated by HeLa cells, we confirmed the expression of HLA-G mRNA in primary cultured conjunctival and limbal cells by RT-PCR and Western blots. Conjunctival cells expressed significantly higher levels of HLA-G on AM- than on collagen-coated dishes when measured by real-time PCR. The same trend was observed in limbal cells; however, the difference was not statistically significant. The upregulation of HLA-G was not a contamination by native AM RNA, because the AM used in the study was extensively processed to remove cellular components, and RT-PCR of AM samples alone did not yield any RNA bands.

According to another report, immunohistochemical analysis carried out on corneas showed positive immunohistochemical staining with anti–HLA-G antibodies.[35] However, we were not able to detect HLA-G in cornea tissue sections (data not shown) or cytospin samples of epithelial cells by immunohistochemistry. Western blot analysis detected the HLA-G protein only in cultured cells as well. HLA-G was also detected in primary cultured limbal epithelial cells (Fig. 3). This discrepancy may be caused by different epitopes recognized by the antibodies used. However, because HLA-G

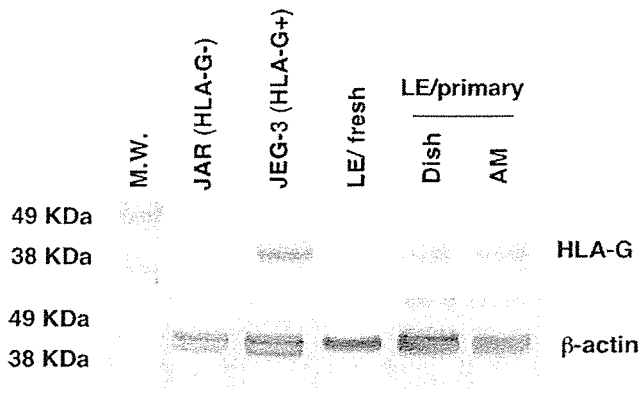

FIGURE 4. Western blot of HLA-G protein in limbal epithelium and primary cultured LE cells expanded on plastic and AM. Samples were loaded with 20 mg of protein/lane. HLA-G protein was detected in cultured LE, but not in freshly dissociated limbal epithelium. β-actin was run as internal control. JAR, HLA-G–negative control; JEG-3, HLA-G–positive control.

mRNA was detected in freshly dissociated cells by RT-PCR, it is possible that the cornea may express HLA-G in vivo under inflammatory conditions. The staining pattern of HLA-G in cytospin samples and primary cultures (Fig. 3) was not strictly localized to the cell membrane as shown in the placenta-positive control. This result may have been caused by incomplete trafficking of HLA-G to the cell membrane in corneal epithelial cells.

We showed that gene transfer of cornea-derived HLA-G into K-562 cells slightly inhibited lysis by NK cells in vitro. This effect was also shown in another study,[26] as well as in HLA-G transfected primary human myoblasts.[34] This model was used because K-562 cells are void of membrane-bound HLA molecules, allowing for the analysis of HLA-G alone, without the involvement of other HLA molecules. The results suggest that HLA-G expressed on cultivated sheets may block the lytic activity of NK cells after transplantation to the ocular surface. There are reports that suggest the involvement of NK cells in allograft rejection after keratoplasty in rodents.[36,37] Clinically, soluble HLA-G levels in serum and biopsy samples were shown to correlate with graft survival in cardiac transplant patients.[38] Although our results did not reach statistical significance, this may have been caused by inadequate protein upregulation by transfection. However, the objective of this experiment was to show partial functional upregulation by transfection of the *HLA-G* gene obtained directly from corneal epithelial cells.

Cultivated sheet transplantation has become another tool in the treatment of ocular surface disease. AM is often used as a carrier; however, other substrates such as fibrin[39] and temperature-sensitive polymers[40] have been reported. It is possible that the upregulation of HLA-G is not a specific response to AM carriers; however, a statistically greater enhancement was observed in conjunctival cells in our study. Although further studies are required to elucidate the precise mechanisms involved, HLA-G upregulation may be an advantage of ex vivo cultivated sheets over direct transplantation of epithelial tissue.

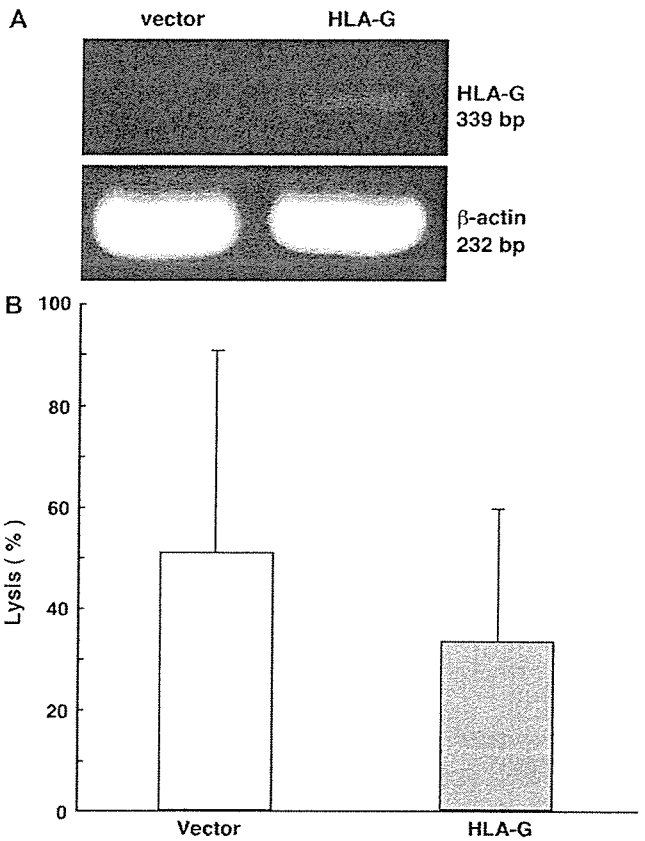

FIGURE 5. Class 1–negative K562 cells were transfected with an HLA-G construction vector or a vector-only negative control. (A), RT-PCR of HLA-G in transfectants. (B), Cytolysis of K562 cells by CD56+ NK cells was inhibited by HLA-G expression. Data are expressed as mean ± SD (n = 4).

ACKNOWLEDGMENTS

The authors thank Mifuyu Oshima and Hiroe Fujikawa for technical assistance and the staff of the Cornea Center Eye Bank for administrative support.

REFERENCES

1. Kim JC, Tseng SC. Transplantation of preserved human amniotic membrane for surface reconstruction in severely damaged rabbit corneas. *Cornea*. 1995;14:473–484.
2. Tsubota K, Satake Y, Ohyama M, et al. Surgical reconstruction of the ocular surface in advanced ocular cicatricial pemphigoid and Stevens-Johnson syndrome. *Am J Ophthalmol*. 1996;122:38–52.
3. Shimazaki J, Yang HY, Tsubota K. Amniotic membrane transplantation for ocular surface reconstruction in patients with chemical and thermal burns. *Ophthalmology*. 1997;104:2068–2076.
4. Tseng SC, Prabhasawat P, Barton K, et al. Amniotic membrane transplantation with or without limbal allografts for corneal surface reconstruction in patients with limbal stem cell deficiency. *Arch Ophthalmol*. 1998;116:431–441.
5. Koizumi N, Inatomi T, Quantock AJ, et al. Amniotic membrane as a substrate for cultivating limbal corneal epithelial cells for autologous transplantation in rabbits. *Cornea*. 2000;19:65–71.
6. Nakamura T, Endo K, Cooper LJ, et al. The successful culture and autologous transplantation of rabbit oral mucosal epithelial cells on amniotic membrane. *Invest Ophthalmol Vis Sci*. 2003;44:106–116.

7. Fortunato SJ, Menon R, Lombardi SJ. Interleukin-10 and transforming growth factor-beta inhibit amniochorion tumor necrosis factor-alpha production by contrasting mechanisms of action: therapeutic implications in prematurity. *Am J Obstet Gynecol.* 1997;177:803–809.
8. Yam HF, Pang CP, Fan DS, et al. Growth factor changes in ex vivo expansion of human limbal epithelial cells on human amniotic membrane. *Cornea.* 2002;21:101–105.
9. Tseng SC, Li DQ, Ma X. Suppression of transforming growth factor-beta isoforms, TGF-beta receptor type II, and myofibroblast differentiation in cultured human corneal and limbal fibroblasts by amniotic membrane matrix. *J Cell Physiol.* 1999;179:325–335.
10. Kim JS, Kim JC, Na BK, et al. Amniotic membrane patching promotes healing and inhibits proteinase activity on wound healing following acute corneal alkali burn. *Exp Eye Res.* 2000;70:329–337.
11. Shimmura S, Shimazaki J, Ohashi Y, et al. Antiinflammatory effects of amniotic membrane transplantation in ocular surface disorders. *Cornea.* 2001;20:408–413.
12. Higa K, Shimmura S, Shimazaki J, et al. Hyaluronic acid-CD 44 interaction mediates the adhesion of lymphocytes by amniotic membrane stroma. *Cornea.* 2005;24:206–212.
13. Ma DH, Yao JY, Yeh LK, et al. In vitro antiangiogenic activity in ex vivo expanded human limbocorneal epithelial cells cultivated on human amniotic membrane. *Invest Ophthalmol Vis Sci.* 2004;45:2586–2595.
14. Shao C, Sima J, Zhang SX, et al. Suppression of corneal neovascularization by PEDF release from human amniotic membranes. *Invest Ophthalmol Vis Sci.* 2004;45:1758–1762.
15. Kobayashi N, Kabuyama Y, Sasaki S, et al. Suppression of corneal neovascularization by culture supernatant of human amniotic cells. *Cornea.* 2002;21:62–67.
16. Sionov RV, Yagel S, Har-Nir R, et al. Trophoblasts protect the inner cell mass from macrophage destruction. *Biol Reprod.* 1993;49:588–595.
17. Beer AE, Sio JO. Placenta as an immunological barrier. *Biol Reprod.* 1982;26:15–27.
18. Ueta M, Kweon MN, Sano Y, et al. Immunosuppressive properties of human amniotic membrane for mixed lymphocyte reaction. *Clin Exp Immunol.* 2002;129:464–470.
19. Shimazaki J, Aiba M, Goto E, et al. Transplantation of human limbal epithelium cultivated on amniotic membrane for the treatment of severe ocular surface disorders. *Ophthalmology.* 2002;109:1285–1290.
20. Bainbridge DR. Evolution of mammalian pregnancy in the presence of the maternal immune system. *Rev Reprod.* 2000;5:67–74.
21. Chumbley G, King A, Holmes N, et al. In situ hybridization and northern blot demonstration of HLA-G mRNA in human trophoblast populations by locus-specific oligonucleotide. *Hum Immunol.* 1993;37:17–22.
22. Ellis SA, Palmer MS, McMichael AJ. Human trophoblast and the choriocarcinoma cell line BeWo express a truncated HLA Class I molecule. *J Immunol.* 1990;144:731–735.
23. King A, Allan DS, Bowen M, et al. HLA-E is expressed on trophoblast and interacts with CD94/NKG2 receptors on decidual NK cells. *Eur J Immunol.* 2000;30:1623–1631.
24. King A, Burrows TD, Hiby SE, et al. Surface expression of HLA-C antigen by human extravillous trophoblast. *Placenta.* 2000;21:376–387.
25. King A, Boocock C, Sharkey AM, et al. Evidence for the expression of HLAA-C class I mRNA and protein by human first trimester trophoblast. *J Immunol.* 1996;156:2068–2076.
26. Rouas-Freiss N, Goncalves RM, Menier C, et al. Direct evidence to support the role of HLA-G in protecting the fetus from maternal uterine natural killer cytolysis. *Proc Natl Acad Sci USA.* 1997;94:11520–11525.
27. Pazmany L, Mandelboim O, Vales-Gomez M, et al. Protection from natural killer cell-mediated lysis by HLA-G expression on target cells. *Science.* 1996;274:792–795.
28. Munz C, Holmes N, King A, et al. Human histocompatibility leukocyte antigen (HLA)-G molecules inhibit NKAT3 expressing natural killer cells. *J Exp Med.* 1997;185:385–391.
29. Perez-Villar JJ, Melero I, Navarro F, et al. The CD94/NKG2-A inhibitory receptor complex is involved in natural killer cell-mediated recognition of cells expressing HLA-G1. *J Immunol.* 1997;158:5736–5743.
30. Pende D, Sivori S, Accame L, et al. HLA-G recognition by human natural killer cells. Involvement of CD94 both as inhibitory and as activating receptor complex. *Eur J Immunol.* 1997;27:1875–1880.
31. Soderstrom K, Corliss B, Lanier LL, et al. CD94/NKG2 is the predominant inhibitory receptor involved in recognition of HLA-G by decidual and peripheral blood NK cells. *J Immunol.* 1997;159:1072–1075.
32. Yang Y, Chu W, Geraghty DE, et al. Expression of HLA-G in human mononuclear phagocytes and selective induction by IFN-gamma. *J Immunol.* 1996;156:4224–4231.
33. Moreau P, Adrian-Cabestre F, Menier C, et al. IL-10 selectively induces HLA-G expression in human trophoblasts and monocytes. *Int Immunol.* 1999;11:803–811.
34. Wiendl H, Mitsdoerffer M, Hofmeister V, et al. The non-classical MHC molecule HLA-G protects human muscle cells from immune-mediated lysis: implications for myoblast transplantation and gene therapy. *Brain.* 2003;126:176–185.
35. Le Discorde M, Moreau P, Sabatier P, et al. Expression of HLA-G in human cornea, an immune-privileged tissue. *Hum Immunol.* 2003;64:1039–1044.
36. Larkin DF, Calder VL, Lightman SL. Identification and characterization of cells infiltrating the graft and aqueous humour in rat corneal allograft rejection. *Clin Exp Immunol.* 1997;107:381–391.
37. Claerhout I, Kestelyn P, Debacker V, et al. Role of natural killer cells in the rejection process of corneal allografts in rats. *Transplantation.* 2004;77:676–682.
38. Lila N, Carpentier A, Amrein C, et al. Implication of HLA-G molecule in heart-graft acceptance. *Lancet.* 2000;355:2138.
39. Rama P, Bonini S, Lambiase A, et al. Autologous fibrin-cultured limbal stem cells permanently restore the corneal surface of patients with total limbal stem cell deficiency. *Transplantation.* 2001;72:1478–1485.
40. Nishida K, Yamato M, Hayashida Y, et al. Functional bioengineered corneal epithelial sheet grafts from corneal stem cells expanded ex vivo on a temperature-responsive cell culture surface. *Transplantation.* 2004;77:379–385.

Cytokeratin 15 Can Be Used to Identify the Limbal Phenotype in Normal and Diseased Ocular Surfaces

Satoru Yoshida,[1,2] *Shigeto Shimmura,*[1,2] *Tetsuya Kawakita,*[3] *Hideyuki Miyashita,*[2] *Seika Den,*[3] *Jun Shimazaki,*[2,3] *and Kazuo Tsubota*[1,2]

Purpose. To elucidate the expression pattern of K15, K19, K14, and K12 in human and mouse ocular surface epithelium as putative markers of epithelial phenotype.

Methods. Immunohistochemical staining with specific antibodies for K15, K19, K14, and K12 was performed in human donor cornea tissue and normal ICR mouse corneas, with emphasis on localization of immunopositive cells. Immunohistochemistry was performed in a limbus-deficient mouse model as well as in clinical samples of pannus surgically removed from a thermal burn and a patient with Saltzmann's dystrophy. Staining patterns were classified as limited to the most basal layer (K^{bas}), basal and suprabasal layers ($K^{bas\text{-}sup}$), predominantly in suprabasal layers (K^{sup}) and negative staining (K^{-}).

Results. In human conjunctival epithelium, strong expression of K15 was observed in basal cells, whereas K19 was expressed in both basal and suprabasal layers ($K15^{bas}/K19^{bas\text{-}sup}/K12^{-}$). Limbal epithelial cells were $K15^{bas\text{-}sup}/K19^{bas\text{-}sup}/K12^{sup}$, whereas epithelial cells in the central cornea were $K15^{-}/K19^{bas\text{-}sup}/K12^{bas\text{-}sup}$. In contrast, the mouse ocular surface demonstrated a different expression pattern of K15 and K19 than did the human tissue in the conjunctiva ($K15^{bas\text{-}sup}/K19^{bas}/K12^{-}$) and the limbus ($K15^{bas\text{-}sup}/K19^{bas}/K12^{sup}$). Neither K15 nor K19 was expressed in the central mouse cornea ($K15^{-}/K19^{-}/K12^{bas\text{-}sup}$). Similar cytokeratin expression was observed in conjunctivalized corneas in mice and in surgically removed pannus tissue.

Conclusions. Although the expression of K15 and K19 differ in humans and mice, specific staining patterns can be used to characterize the epithelial phenotype in normal and diseased ocular surface. (*Invest Ophthalmol Vis Sci.* 2006;47: 4780–4786) DOI:10.1167/iovs.06-0574

Keratins (cytokeratins and hair keratins) are a family of cytoskeletal component proteins of epithelial cells. Cytokeratins are divided into two subfamilies: type I (acidic) and type II (basic to neutral). Usually, at least one member of the type I family and one member of the type II family are coordinately expressed in each epithelial cell, and together they form intermediate filaments responsible for the structural integrity of epithelial cells.[1,2] Cytokeratins also seem to play a critical role in tissue differentiation, and the different patterns of cytokeratin expression in epithelia is often used as markers of differentiation.[3–5] For example, it is widely known that differentiated human corneal epithelial cells express cytokeratin 3 (K3, type II) and K12 (type I).[6–9] The cornea-specific expression of K12 has also been found in mice.[10–12] In addition to the predominant expression of K3 and K12, other cytokeratins including K14 and K19 are expressed as minor components of the cytoskeleton in basal and/or suprabasal human corneal epithelial cells.[2,6,13–15]

In the skin, K19 has been proposed as a marker for stem cells in the skin hair follicle and also for proliferative keratinocytes in the basal layer.[16,17] In human ocular surface epithelia, K19 is a minor cytoskeletal component of the corneal epithelium, but it is one of the major components in the conjunctival epithelium where K19 expression is reported to be uniform.[2,6,13–15,18,19] Several studies have reported that K19 expression is found in all layers of the limbal epithelium, which becomes patchy progressively toward the center of the cornea and finally disappears in the center.[2,6,15] K14/K5 expression is believed to be a marker for mitotically active, proliferative basal cells of stratified epithelia.[7] Indeed, K14 expression in the basal layer of corneal epithelium has been reported in humans, mice, and rats.[7,11,14,20] K15 is another type I cytokeratin expressed in stratified epithelia, with several histologic studies reporting the basal expression of K15 in the epidermis.[21–25] Kasper et al.[6] detected K15 protein in corneal and conjunctival epithelium by two-dimensional gel electrophoresis[6]; however, the localization of K15 in ocular surface epithelia remains unknown.

In the present study, K15 was expressed by limbal and conjunctival epithelia, but not by corneal epithelium, in both humans and mice. Furthermore, human limbal epithelium uniquely showed $K15^{+}$ cells in the suprabasal layers, allowing the distinction of the limbus from conjunctiva. The limbal phenotype can further be characterized by multiple staining with K19 and K12. The pattern of K15 expression, together with other known markers such as ABCG2,[24–26] Cx43,[26,27] and vimentin,[6,14,28,29] can be used to identify basal cells of the limbal area in normal and diseased tissue.

Material and Methods

Mouse Corneas

Specific pathogen-free adult ICR mice (n = 10) were purchased from CLEA Japan, Inc., Tokyo, Japan). All animals were handled in full accordance with the ARVO Statement for the Use of Animals in Ophthalmic and Vision Research and institutional guidelines. To produce total limbal deficiency, we denuded the corneal epithelium including the limbal area with an ophthalmic knife. Re-epithelialization of the scraped cornea was monitored by fluorescein staining. In another group of mice, the ocular surface was air dried for 15 minutes at room temperature under topical anesthesia. After 2 to 4 weeks, the mice were killed by cervical dislocation and the eyes were excised and

From the [1]Cornea Center and the [3]Department of Ophthalmology, Tokyo Dental College, Chiba, Japan; and the [2]Department of Ophthalmology, Keio University School of Medicine, Tokyo, Japan.

Supported in part by a grant from the Advanced and Innovational Research Program in Life Sciences from the Ministry of Education, Culture, Sports, Science and Technology (TK), and a Grant-in-Aid for Scientific Research (SS).

Submitted for publication May 27, 2006; revised July 3, 2006; accepted August 30, 2006.

Disclosure: **S. Yoshida**, None; **S. Shimmura**, None; **T. Kawakita**, None; **H. Miyashita**, None; **S. Den**, None; **J. Shimazaki**, None; **K. Tsubota**, None

The publication costs of this article were defrayed in part by page charge payment. This article must therefore be marked "*advertisement*" in accordance with 18 U.S.C. §1734 solely to indicate this fact.

Corresponding author: Shigeto Shimmura, Keio University School of Medicine, 35 Shinanomachi, Shinjuku-ku, Tokyo 160-8582, Japan; shige@sc.itc.keio.ac.jp.

Investigative Ophthalmology & Visual Science, November 2006, Vol. 47, No. 11

TABLE 1. Antibodies Used in the Study

Antigen	Clone Name/Code	Type	Host	Immunogen	Manufacturer
K12	sc-17101 (L-15)	Polyclonal	Goat	Mouse K12	Santa Cruz Biotechnology, Santa Cruz, CA
K15	LHK15	Monoclonal	Mouse	Human K15	Lab Vision, Fremont, CA
K15	PCK-153P	Polyclonal	Chicken	Human K15	CRP, Denver, CO
K19	RCK108	Monoclonal	Mouse	Human K19	Lab Vision Corp.
K19	RB-9021	Polyclonal	Rabbit	Human K19	Lab Vision Corp.
K19	A53-B/A2.26	Monoclonal	Mouse	Human K19	Chemicon International, Inc., Temecula, CA
K14	PRB-155P	Polyclonal	Rabbit	Mouse K14	CRP
K14	LL001*	Monoclonal	Mouse	Human K14	Abcam Inc., Cambridge MA
K14	SPK14.2*	Monoclonal	Mouse	Human K14	Abcam Inc.
K5	XM26*	Monoclonal	Mouse	Human K5	Abcam Inc.
K5	PRB-160P*	Polyclonal	Rabbit	Mouse K5	CRP

* Used in Supplementary Figure S1, http://www.iovs.org/cgi/content/full/47/11/4780/DC1.

embedded in 4% carboxy methyl cellulose (CMC; Finetec Co., Ltd., Tokyo, Japan) for immunohistochemical staining. Normal, untreated mice were used as the control.

Human Cornea Samples

Normal human corneas (n = 9) were obtained from Northwest Lions Eye Bank (Seattle, WA) and used as the normal control for immunohistochemistry. Clinical samples of pannus tissue were obtained during surgery from a thermal burn patient and a patient with Saltzmann's nodular degeneration. Written informed consent was obtained from each patient before surgery. Excised tissue was immediately embedded in OCT compound (Tissue-Tek; Sakura Finetek, Co. Ltd., Tokyo, Japan) and prepared for immunohistochemistry. The study protocols involving patients and donor eyes were in compliance with the Declaration of Helsinki.

Immunohistochemistry

Immunocytochemistry was performed as described previously.[30] In brief, whole mouse eye or segments of human sclerocorneal tissue were embedded in 4% CMC. Fresh frozen sections (5–10 μm thick) were air dried, fixed in 4% paraformaldehyde for 10 minutes, and then incubated in fixative (Morphosave; Ventana Medical Systems, Tucson, AZ) for 15 minutes. Blocking was performed with 10% donkey or goat serum in phosphate-buffered saline (PBS) for 30 minutes. Sections were then incubated with primary antibodies for 1 hour at room temperature. The primary antibodies used in this study are summarized in Table 1. Immunoreactivity of primary antibodies was visualized with secondary antibodies conjugated with FITC, Cy3 (Jackson ImmunoResearch Laboratories, West Grove, PA) and Alexa 488 (Invitrogen Corp., Carlsbad, CA). After they were washed with PBS, the sections were mounted (Permafluor; Beckman Coulter Inc., Miami, FL). Images were observed by a microscope (Axioplan 2; Carl Zeiss Inc., Thornwood, NY) equipped with a digital camera (Axiocam; Carl Zeiss Inc.). PAS staining was performed according to standard procedures.

Staining patterns of keratin were classified as limited to the most basal layer (K^{bas}), basal and suprabasal layers ($K^{bas\text{-}sup}$), predominantly in suprabasal layers (K^{sup}) and negative staining (K^-).

RESULTS

Cytokeratin Expression on the Human Ocular Surface

We first examined the expression pattern of K15, K19, and K12 on the human ocular surface. As shown in Figures 1B and 2A, strong K15 expression was observed in the basal layer of the conjunctiva, while K19 was expressed in both the basal and suprabasal layers (Fig. 2A). Because K12 was negative (Fig. 1B), the conjunctival epithelial phenotype was $K15^{bas}$/$K19^{bas\text{-}sup}$/$K12^-$. Further into the limbus, K12 expression appeared mainly in the suprabasal layers, although weak staining was observed in the basal cells as well (Figs. 1D, 1E). K19 expression was similar to that in the conjunctiva; however, K15 staining was distinct from the conjunctiva, with positive cells found in the suprabasal layers as well (Figs. 2A, 2C). The number of $K15^+$ layers varied in different sections, even in samples from the same donor (Figs. 1D, 2C, 2F). The limbal epithelial phenotype can thus be represented as $K15^{bas\text{-}sup}$/

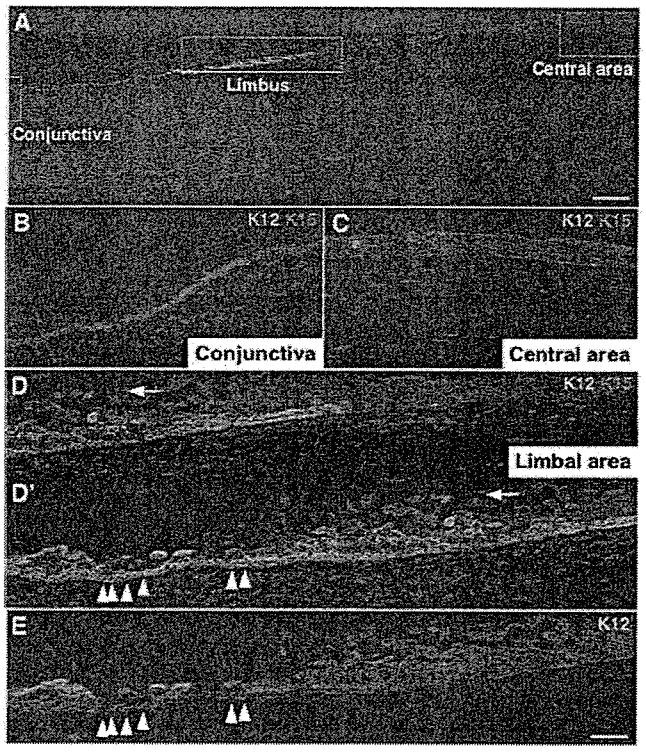

FIGURE 1. Expression of K15 and K12 in human corneal and conjunctival epithelium. (A) An overview of a human ocular surface immunostained with anti-K12 (*green*, FITC) and anti-K15 (*red*, Cy3). *Boxes*: magnified regions shown in conjunctiva (B), central cornea (C), and limbal area (D, D', E). (D, D') Images across the limbus; *white arrow*: same cell in each image. In the conjunctiva, K15 is expressed only in basal cells (B, $K15^{bas}$/$K12^-$). In contrast, $K15^+$ cells were found in the suprabasal layers of the limbus (A, D, D', $K15^{bas\text{-}sup}$/$K12^{sup}$). Isolated $K15^+$ cells were observed in the central area that were also $K12^+$ (C). The expression of K15 was highest in basal cells of the limbal area (D', *arrowheads*). These cells also expressed low levels of K12 (E, *arrowheads*). Scale bar: (A–D') 200 μm; (E) 50 μm.

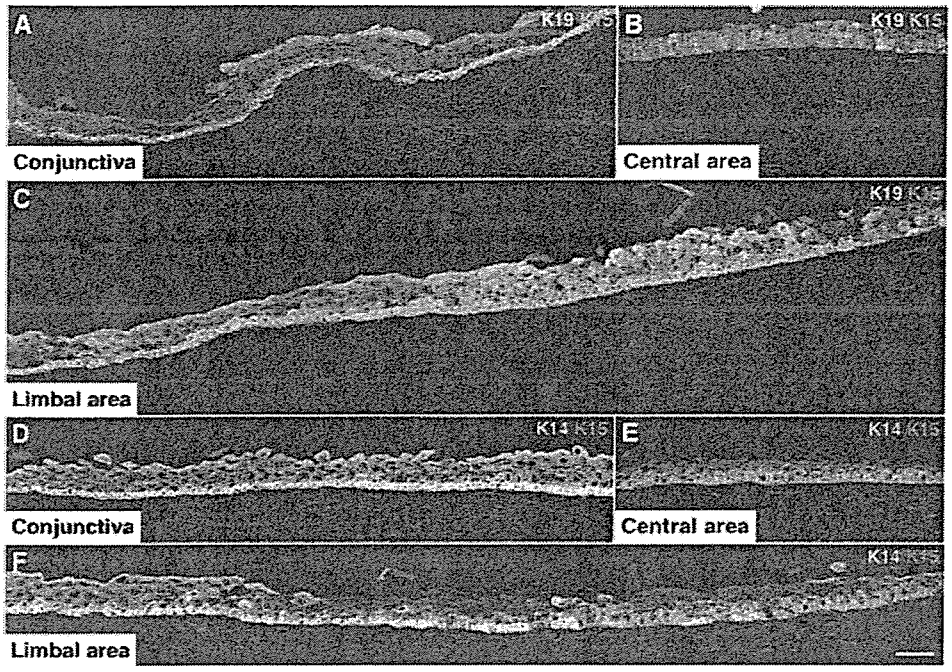

FIGURE 2. Expression pattern of K15, K19, and K14 in human corneal and conjunctival epithelium. Images of serial sections stained with anti-K19 (*green*, FITC) and anti-K15 (*red*, Cy3) antibodies (A–C) and with anti-K14 (*green*) and anti-K15 (*red*) antibodies (D–F). Conjunctiva (A, D) and central (B, E), or limbal area (C, F) of the cornea. Together with the expression of K15, a strong expression of K19 was observed in the basal and suprabasal layers of the conjunctival ($K15^{bas}/K19^{bas\text{-}sup}$) and limbal ($K15^{bas\text{-}sup}/K19^{bas\text{-}sup}$) epithelia (A, C, D, F). Cells weakly positive for K19 were also found in the central area (B, $K15^{-}/K19^{bas\text{-}sup}$). K14 was observed in the conjunctiva and in the basal and suprabasal layers of the limbus and central corneal epithelium (D, E, F). Scale bar, 50 μm.

$K19^{bas\text{-}sup}/K12^{sup}$. The central corneal epithelium was uniformly $K12^{+}$ and $K15^{-}$ (Fig. 1C). In addition, as previously reported by Chen et al.,[31] we found various levels of $K19^{+}$ cells in the central corneal epithelium, although the expression level was lower than in the conjunctiva (Fig. 2B). The phenotype of the central cornea was therefore $K15^{-}/K19^{bas\text{-}sup}/K12^{bas\text{-}sup}$.

We further compared the expression of K15 with that of K14, another basal cell marker. Although K14 expression in the corneal epithelium is considered to be restricted to the basal layer,[11,14,20,28,32] we also found K14 staining in the suprabasal layers of corneal and conjunctival epithelium (Figs. 2D–F). Nevertheless, K14 expression was strongest in the $K15^{+}$ basal cells of the limbal and conjunctival epithelium, as well as in $K15^{-}$ corneal basal cells.

Cytokeratin Expression in the Mouse Ocular Surface

We further examined the expression pattern of cytokeratins in mice, and found a contrasting staining pattern in the conjunctiva compared with human tissue. K15 was expressed in all layers of the conjunctival epithelium (Figs. 3A, 3C, 3D), which was similar to the expression of K19 in human conjunctiva. In contrast, K19 was observed only in the most basal layer of the conjunctival epithelium, mirroring that of K15 expression in humans (Figs. 3B, 3C). In other words, K19 and K15 showed a reciprocal pattern in humans and mice ($K15^{bas\text{-}sup}/K19^{bas}/K12^{-}$). As expected, the limbal epithelium was positive for K12 in the suprabasal layer ($K15^{bas\text{-}sup}/K19^{bas}/K12^{sup}$). Cells from the central to midperipheral cornea were predominantly K15 negative (Figs. 3E–G). K19 staining was also negative in the central mouse cornea (Fig. 3F), whereas K12 was positive in the basal and suprabasal layers ($K15^{-}/K19^{-}/K12^{bas\text{-}sup}$).

The expression pattern of K14 in mouse cornea and conjunctiva was similar to human tissue. Strong expression of K14 was observed in the basal and suprabasal cells from the conjunctiva to the limbus (Figs. 3D, 3G). Suprabasal cells in the central area also expressed K14, but the expression level was weak compared with that in the conjunctiva (Fig. 3G).

Cytokeratin Pattern in Identifying Epithelial Phenotype in Pathologic Tissue

Furthermore, we examine the expression pattern of these cytokeratins in conjunctivalized mouse corneas. Debrided corneal epithelium, as well as corneas subjected to severe drying demonstrated the conjunctival phenotype ($K19^{bas}/K15^{bas\text{-}sup}/K12^{-}$) in the central cornea (Figs. 4A, 4B, 4D). PAS-positive goblet cells were also observed, confirming the conjunctival phenotype (Fig. 4E).

We finally examined the expression pattern of K15, K19, and K12 in two clinical pannus specimens. In the thermal burn patient, excised tissue clearly showed the conjunctival phenotype $K15^{bas}/K19^{bas\text{-}sup}/K12^{-}$ (Fig. 5). In contrast, pannus tissue from the patient with Saltzmann's nodular degeneration showed patchy staining of all 3 cytokeratins (Fig. 6B). High magnification revealed both the conjunctival phenotype $K15^{bas}/K19^{bas\text{-}sup}/K12^{-}$ and the limbal phenotype $K15^{bas\text{-}sup}/K19^{bas\text{-}sup}/K12^{sup}$ in the same field of view (Figs. 6D–F), suggesting that the epithelium extending into the clear cornea includes basal limbal epithelial cells.

DISCUSSION

Several disorders in humans and mice are caused by deficiencies in cytokeratin genes, suggesting that cytoskeletal proteins have important functions in maintaining cellular integrity.[3,3] In addition, cytokeratins are often used in the characterization of epithelial phenotype and differentiation and in the diagnosis of carcinomas. K15 is a type I cytokeratin reported in basal keratinocytes of the epidermis[21] and has also been proposed as a marker of stem cells in the hair follicle bulge.[34,35] However, reports on the expression of K15 in the ocular surface are scarce,[6,21] and the expression pattern remains unclear. In this study, we demonstrated the unique expression pattern of K15 in the basal human and mouse corneal and conjunctival epithelium. Different epithelial phenotypes were shown to express unique patterns of K15, K19, and K12 expression (summarized in Table 2).

FIGURE 3. Expression of K12, K14, K19, and K15 in mouse corneal and conjunctival epithelium. Images of serial sections stained with anti-K12 (*green*, Alexa-488) and anti-K15 (*red*, Cy3) antibodies (**A**, **E**), anti-K12 (*green*) and anti-K19 (*red*) antibodies (**B**), anti-K19 (*green*) and anti-K15 (*red*) antibodies (**C**, **F**), and anti-K14 (*green*) and anti-K15 (*red*) antibodies (**D**, **G**). (**A**–**D**) Limbal area of mouse cornea and conjunctiva. (**E**–**G**) Central area of the cornea. Characteristic keratin expression patterns were observed in the central cornea ($K15^{-}/K19^{-}/K12^{bas\text{-}sup}$), the limbal area ($K15^{bas\text{-}sup}/K19^{bas}/K12^{sup}$), and the conjunctiva ($K15^{bas\text{-}sup}/K19^{bas}/K12^{-}$). As in human tissue, strong expression of K14 was observed in the basal layer of the cornea and suprabasal cells of the conjunctiva (**D**, **G**). Moderate expression of K14 was observed in suprabasal cells in corneal epithelium (**G**). Scale bar, 50 μm.

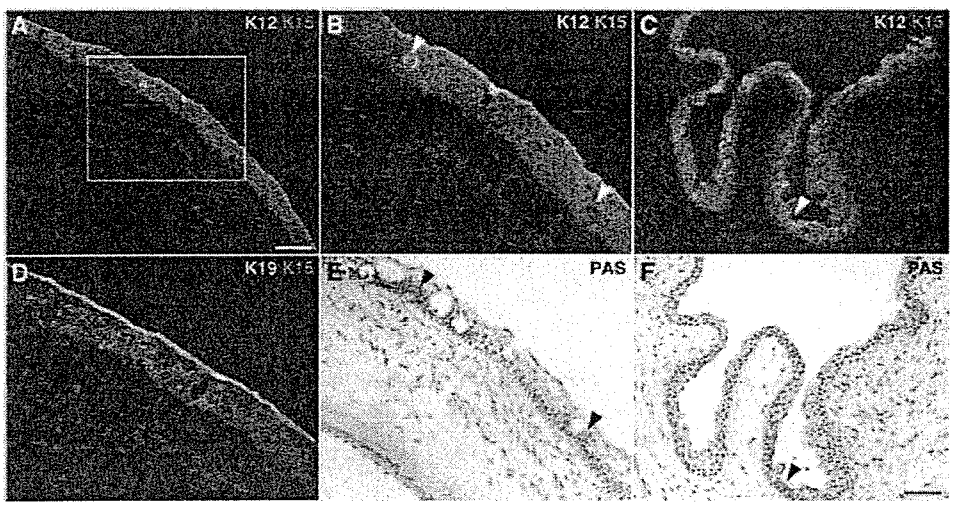

FIGURE 4. Expression of K12, K19, and K15 in conjunctivalized mouse cornea. Sections were stained with anti-K12 (*green*, Alexa-488) and anti-K15 (*red*, Cy3) antibodies (**A**–**C**), anti-K19 (*green*) and anti-K15 (*red*) antibodies (**D**), and PAS (**E**, **F**). (**A**, **B**, **D**, **E**) Central mouse cornea with conjunctivalized epithelium. (**A**) Low-magnification image; *box*: magnified region shown in (**B**). (**C**, **F**) Conjunctival positive control. Conjunctivalization of the cornea is verified by the conjunctival phenotype pattern ($K15^{bas\text{-}sup}/K19^{bas}/K12^{-}$). PAS-positive goblet cells (*black arrowhead*) were also observed (**E**). Background anti-K12 staining was found in goblet cells (*white arrowhead*) in the conjunctiva (**C**) and conjunctivalized cornea epithelium (**B**). Scale bars: (**A**) 100 μm; (**F**) 50 μm.

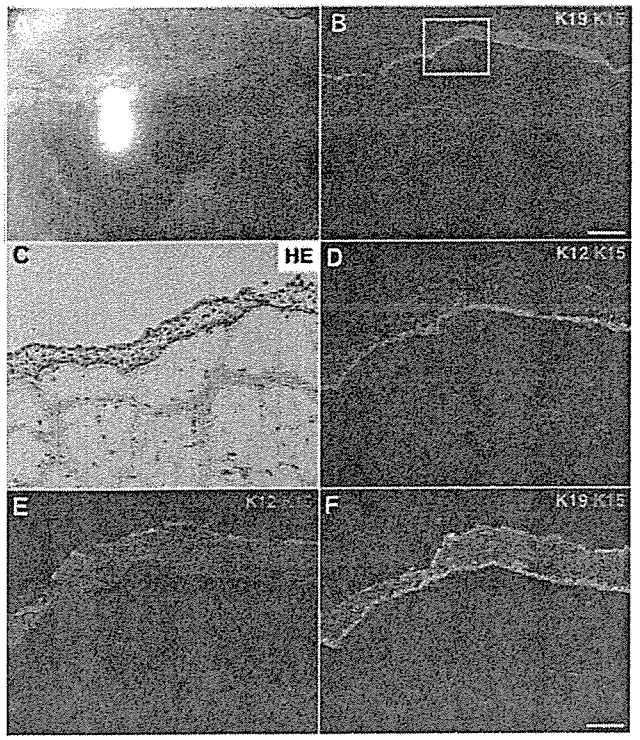

FIGURE 5. Expression of K12, K19, and K15 in a thermal burn patient. (A) Slit micrograph of a vascularized pannus with central corneal phenotype. Hematoxylin-eosin–stained (C) and immunostained (D–F) areas corresponding to the *boxed* region in (B). Serial sections were double stained for K12 (*green*, negative) and K15 (*red*) (D), K12 (*green*, negative) and K19 (*red*) (E), or K19 (*green*) and K15 (*green*) (F). The tissue shows the conjunctiva phenotype $K15^{bas}/K19^{bas\text{-}sup}/K12^{-}$. Scale bars: (B) 200 μm; (F) 50 μm.

It is commonly accepted that in humans, K14 is expressed in the basal layer of the corneal and conjunctival epithelium, and K19 is expressed in basal limbal cells and all layers of the conjunctival epithelium. However, we found K14 in all layers of each stratified epithelia, although the expression level in the suprabasal layers of the corneal epithelium was lower than that in the basal layer. Because the expression of K14 spans the entire length of the ocular surface, it is not useful as a marker to distinguish limbal cells from conjunctival and corneal basal cells. The expression pattern of K19 is also controversial,[19,31] and we found that it is expressed through all layers of the human conjunctival and corneal epithelium, including the limbal area. However, the expression of K19 in the central corneal epithelium showed variation among individuals. Another report by Kasper et al.[6] also showed K19 expressed in all layers of the limbal epithelium.

The difference in the immunohistochemical staining pattern is probably due to variations in technical procedure, which includes the method of tissue processing, the sensitivity of antibodies used, and conditions for visualization. For example, overfixation often leads to loss or reduction of antigen reactivity. Indeed, staining patterns of p63, another gene often used to stain the limbal epithelium, varies greatly in tissue-processing methods.[20] We have confirmed the expression pattern of the cytokeratins demonstrated in this study by using several antibodies for K15, K19, or K14 (Table 1, Supplementary Fig. S1). In addition to K14, we found that K5, a type II partner of K14, is expressed in all layers of the epithelia (Supplementary Fig. S1, online at http://www.iovs.org/cgi/content/full/47/11/4780/DC1), suggesting that the variation in staining mainly depends on the difference in tissue processing rather than the type of antibody used. The condition of the tissue used for immunocytochemistry may also affect keratin expression, because Di Iorio et al.[36] reported that the expression pattern of other stem cell markers depended on the condition of the donor corneas used. However, the elapsed time between death and use of the corneas used in our study was standardized at approximately 5 days (range, 3.5–8.5), and samples were fixed immediately after use for surgery. The variation of cytokeratin expression did not seem to be associated with the variation in elapsed time from death, but rather on the location within a specific sample.

Recently, Kawasaki et al.[37] reported that the K12-positive cells appear to be ectopically residing, self-maintaining corneal epithelial cells in the conjunctival epithelium. We were unable to find such cells in our samples, probably because we did not specifically look for such cell clusters. However, it would be interesting to re-examine such K12-positive clusters in the conjunctiva for K15 expression in the basal and suprabasal layers.

In mice, although expression of K12 and K14 was similar to that in human tissue, strong expression of K15 and K19 was found respectively in the suprabasal and basal layers of the limbal and conjunctival epithelium. The expression pattern of K15 and K19 in mice was exactly the opposite of what was found in human tissue. The data suggest that the functions of these cytokeratins are switched between both species. Both K15 and K19 are type I acidic cytokeratins with undefined type II partners. Because K15 and K19 are not expressed in the

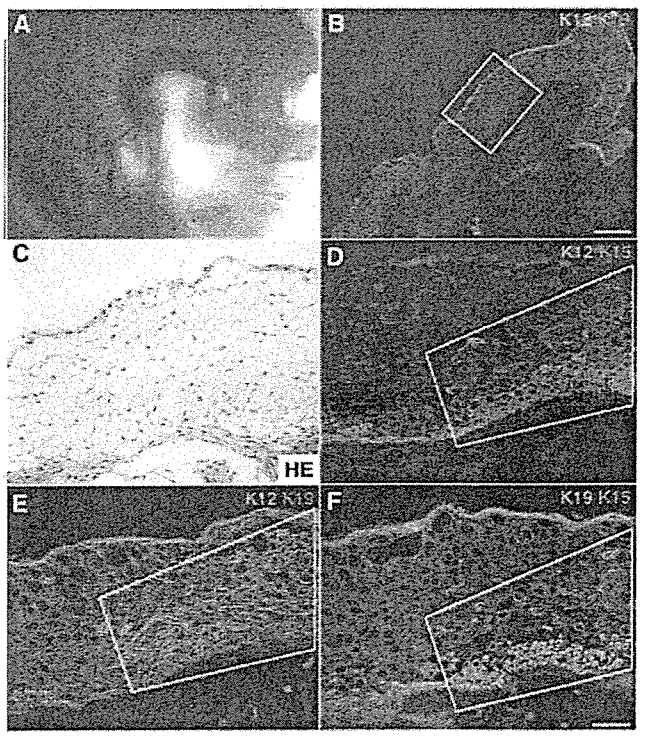

FIGURE 6. Expression of K12, K19, and K15 in a Saltzmann's nodular degeneration patient. (A) Presurgical slit micrograph of the pannus extending from the inferior nasal quadrant of the right eye. Hematoxylin-eosin–stained (C) and immunostained (D–F) images of the area corresponding to the *boxed* region in (B). Serial sections were double stained for K12 (*green*, negative) and K15 (*red*) (D), K12 (*green*, negative) and K19 (*red*) (E), or K19 (*green*) and K15 (*green*) (F). Both the conjunctival phenotype $K15^{bas}/K19^{bas\text{-}sup}/K12^{-}$ and limbal phenotype $K15^{bas\text{-}sup}/K19^{bas\text{-}sup}/K12^{sup}$ (D–F, *boxes*) were observed in this tissue. Scale bar, 50 μm.

TABLE 2. Summary of K12, K14, K15, and K19 Expression in Human and Mouse Ocular Surface Epithelium

	Conjunctiva		Limbal Area		Central Area	
	Basal	Suprabasal	Basal	Suprabasal	Basal	Suprabasal
Human	$K15^{bas}/K19^{bas\text{-}sup}/K12^{-}$		$K15^{bas\text{-}sup}/K19^{bas\text{-}sup}/K12$		$K15^{-}/K19^{bas\text{-}sup}/K12^{bas\text{-}sup}$	
K12	−	−	+/−	+/−	++	++
K15	+++	−	+++*	++/+/−*	−†	−†
K19	+++	++	+++	++	+	+
K14	+++	++	+++	++	+++	
Mouse	$K15^{bas\text{-}sup}/K19^{bas}/K12^{-}$		$K15^{bas\text{-}sup}/K19^{bas}/K12^{sup}$		$K15^{-}/K19^{-}/K12^{bas\text{-}sup}$	
K12	−	−	+/−	+/−	++	++
K15	+	++	+	++	−	−
K19	++	−‡	++	−‡	−	−
K14	+++	++	+++	++	+++	+

* The number of K15-positive cells vary in different sections.
† Occasional positive cell.
‡ Background staining.

central cornea ($K15^{-}/K19^{-}/K12^{bas\text{-}sup}$), both can be used to demonstrate conjunctivalization in mice. The possibility that antibodies for K15 and K19 cross-react respectively with K19 and K15 in mice cannot be completely ruled out. However, this is highly unlikely when the amino acid sequences of the cytokeratins are compared in both species.

Although cytokeratin expression alone is not sufficient to identify stem cells or transient amplifying (TA) cells, the expression profile of several key cytokeratins can be used to characterize epithelial phenotype in normal and diseased tissue. We have also identified K15 as a key cytokeratin that, unlike K14, is not expressed in differentiated corneal epithelium, and can also be used to differentiate limbal phenotype from the conjunctiva. Indeed, the human limbal phenotype $K15^{bas\text{-}sup}/K19^{bas\text{-}sup}/K12^{sup}$ was found in surgically removed tissue that was clinically diagnosed as invading conjunctival epithelium. Therefore, this staining combination may be used to identify residual limbal structures in limbal deficient eyes.

Acknowledgments

The authors thank Kimie Kato for technical assistance.

References

1. Irvine AD, McLean WH. Human keratin diseases: the increasing spectrum of disease and subtlety of the phenotype-genotype correlation. *Br J Dermatol.* 1999;140:815–828.
2. Pitz S, Moll R. Intermediate-filament expression in ocular tissue. *Prog Retin Eye Res.* 2002;21:241–262.
3. Fuchs E. Keratins as biochemical markers of epithelial differentiation. *Trends Genet.* 1988;4:277–281.
4. Sun TT, Eichner R, Nelson WG, et al. Keratin classes: molecular markers for different types of epithelial differentiation. *J Invest Dermatol.* 1983;81:109S–115S.
5. Tseng SC, Jarvinen MJ, Nelson WG, et al. Correlation of specific keratins with different types of epithelial differentiation: monoclonal antibody studies. *Cell.* 1982;30:361–372.
6. Kasper M, Moll R, Stosiek P, Karsten U. Patterns of cytokeratin and vimentin expression in the human eye. *Histochemistry.* 1988;89:369–377.
7. Moll R, Franke WW, Schiller DL, Geiger B, Krepler R. The catalog of human cytokeratins: patterns of expression in normal epithelia, tumors and cultured cells. *Cell.* 1982;31:11–24.
8. Sun TT, Tseng SC, Huang AJ, et al. Monoclonal antibody studies of mammalian epithelial keratins: a review. *Ann NY Acad Sci.* 1985;455:307–329.
9. Tanifuji-Terai N, Terai K, Hayashi Y, Chikama T, Kao WW. Expression of keratin 12 and maturation of corneal epithelium during development and postnatal growth. *Invest Ophthalmol Vis Sci.* 2006;47:545–551.
10. Kao WW, Liu CY, Converse RL, et al. Keratin 12-deficient mice have fragile corneal epithelia. *Invest Ophthalmol Vis Sci.* 1996;37:2572–2584.
11. Kurpakus MA, Maniaci MT, Esco M. Expression of keratins K12, K4 and K14 during development of ocular surface epithelium. *Curr Eye Res.* 1994;13:805–814.
12. Liu CY, Zhu G, Westerhausen-Larson A, et al. Cornea-specific expression of K12 keratin during mouse development. *Curr Eye Res.* 1993;12:963–974.
13. Elder MJ, Hiscott P, Dart JK. Intermediate filament expression by normal and diseased human corneal epithelium. *Hum Pathol.* 1997;28:1348–1354.
14. Kasper M, Stosiek P, Lane B. Cytokeratin and vimentin heterogeneity in human cornea. *Acta Histochem.* 1992;93:371–381.
15. Kivela T, Uusitalo M. Structure, development and function of cytoskeletal elements in non-neuronal cells of the human eye. *Prog Retin Eye Res.* 1998;17:385–428.
16. Lyle S, Christofidou-Solomidou M, Liu Y, et al. The C8/144B monoclonal antibody recognizes cytokeratin 15 and defines the location of human hair follicle stem cells. *J Cell Sci.* 1998;111:3179–3188.
17. Michel M, Torok N, Godbout MJ, et al. Keratin 19 as a biochemical marker of skin stem cells in vivo and in vitro: keratin 19 expressing cells are differentially localized in function of anatomic sites, and their number varies with donor age and culture stage. *J Cell Sci.* 9:1017–.
18. Espana EM, Di Pascuale MA, He H, et al. Characterization of corneal pannus removed from patients with total limbal stem cell deficiency. *Invest Ophthalmol Vis Sci.* 2004;45:2961–2966.
19. Schlotzer-Schrehardt U, Kruse FE. Identification and characterization of limbal stem cells. *Exp Eye Res.* 2005;81:247–264.
20. Hsueh YJ, Wang DY, Cheng CC, Chen JK. Age-related expressions of p63 and other keratinocyte stem cell markers in rat cornea. *J Biomed Sci.* 2004;11:641–651.
21. Lloyd C, Yu QC, Cheng J, et al. The basal keratin network of stratified squamous epithelia: defining K15 function in the absence of K14. *J Cell Biol.* 1995;129:1329–1344.
22. Porter RM, Lunny DP, Ogden PH, et al. K15 expression implies lateral differentiation within stratified epithelial basal cells. *Lab Invest.* 2000;80:1701–1710.
23. Waseem A, Dogan B, Tidman N, et al. Keratin 15 expression in stratified epithelia: downregulation in activated keratinocytes. *J Invest Dermatol.* 1999;112:362–369.
24. Budak MT, Alpdogan OS, Zhou M, et al. Ocular surface epithelia contain ABCG2-dependent side population cells exhibiting features associated with stem cells. *J Cell Sci.* 2005;118:1715–1724.
25. Watanabe K, Nishida K, Yamato M, et al. Human limbal epithelium contains side population cells expressing the ATP-binding cassette transporter ABCG2. *FEBS Lett.* 2004;565:6–10.

26. Wołosin JM, Budak MT, Akinci MA. Ocular surface epithelial and stem cell development. *Int J Dev Biol.* 2004;48:981–991.
27. Matic M, Petrov IN, Chen S, et al. Stem cells of the corneal epithelium lack connexins and metabolite transfer capacity. *Differentiation.* 1997;61:251–260.
28. Kasper M. Patterns of cytokeratins and vimentin in guinea pig and mouse eye tissue: evidence for regional variations in intermediate filament expression in limbal epithelium. *Acta Histochem.* 1992; 93:319–332.
29. Lauweryns B, van den Oord JJ, Missotten L. The transitional zone between limbus and peripheral cornea: an immunohistochemical study. *Invest Ophthalmol Vis Sci.* 1993;34:1991–999.
30. Yoshida S, Shimmura S, Shimazaki J, Shinozaki N, Tsubota K. Serum-free spheroid culture of mouse corneal keratocytes. *Invest Ophthalmol Vis Sci.* 2005;46:1653–658.
31. Chen Z, de Paiva CS, Luo L, et al. Characterization of putative stem cell phenotype in human limbal epithelia. *Stem Cells.* 2004;22: 355–366.
32. Kasper M. Heterogeneity in the immunolocalization of cytokeratin specific monoclonal antibodies in the rat eye: evaluation of unusual epithelial tissue entities. *Histochemistry.* 1991;95:613–620.
33. Porter RM, Lane EB. Phenotypes, genotypes and their contribution to understanding keratin function. *Trends Genet.* 2003;19:278–285.
34. Liu Y, Lyle S, Yang Z, Cotsarelis G. Keratin 15 promoter targets putative epithelial stem cells in the hair follicle bulge. *J Invest Dermatol.* 2003;121:963–968.
35. Morris RJ, Liu Y, Marles L, et al. Capturing and profiling adult hair follicle stem cells. *Nat Biotechnol.* 2004;22:411–.
36. Di Iorio E, Barbaro V, Ruzza A, et al. Isoforms of DeltaNp63 and the migration of ocular limbal cells in human corneal regeneration. *Proc Natl Acad Sci USA.* 2005;102:9523–9528.
37. Kawasaki S, Tanioka H, Yamasaki K, et al. Clusters of corneal epithelial cells reside ectopically in human conjunctival epithelium. *Invest Ophthalmol Vis Sci.* 2006;47:1359–1367.

STEM CELLS
TISSUE-SPECIFIC STEM CELLS

Isolation of Multipotent Neural Crest-Derived Stem Cells from the Adult Mouse Cornea

SATORU YOSHIDA,[a,b] SHIGETO SHIMMURA,[a,b] NARIHITO NAGOSHI,[c] KEIICHI FUKUDA,[d] YUMI MATSUZAKI,[c] HIDEYUKI OKANO,[c] KAZUO TSUBOTA[a,b]

[a]Cornea Center, Tokyo Dental College, Ichikawa, Chiba, Japan; [b]Department of Ophthalmology, Keio University School of Medicine, Shinjuku-ku, Tokyo, Japan; [c]Department of Physiology, Keio University School of Medicine, Shinjuku-ku, Tokyo, Japan; [d]Department of Regenerative Medicine and Advanced Cardiac Therapeutics, Keio University School of Medicine, Shinjuku-ku, Tokyo, Japan

Key Words. Corneal stroma • Keratocyte • Stem cells • Bone marrow cells • Neural crest

ABSTRACT

We report the presence of neural crest-derived corneal precursors (COPs) that initiate spheres by clonal expansion from a single cell. COPs expressed the stem cell markers *nestin*, *Notch1*, *Musashi-1*, and *ABCG2* and showed the side population cell phenotype. COPs were multipotent with the ability to differentiate into adipocytes, chondrocytes, as well as neural cells, as shown by the expression of β-III-tubulin, glial fibrillary acidic protein, and neurofilament-M. COP spheres prepared from E/nestin-enhanced green fluorescent protein (EGFP) mice showed induction of EGFP expression that was not originally observed in the cornea, indicating activation of the neural-specific nestin second intronic enhancer in culture. COPs were Sca-1$^+$, CD34$^+$, CD45$^-$, and c-kit$^-$. Numerous GFP$^+$ cells were observed in the corneas of mice transplanted with whole bone marrow of transgenic mice ubiquitously expressing GFP; however, no GFP$^+$ COP spheres were initiated from these mice. On the other hand, COP spheres from transgenic mice encoding P0-Cre/Floxed-EGFP as well as Wnt1-Cre/Floxed-EGFP were GFP$^+$, indicating the neural crest origin of COPs, which was confirmed by the expression of the embryonic neural crest markers *Twist*, *Snail*, *Slug*, and *Sox9*. Taken together, these data indicate the existence of neural crest-derived, multipotent stem cells in the adult cornea. STEM CELLS *2006;24:2714–2722*

INTRODUCTION

The cornea is an avascular, structurally unique tissue that functions as the primary refracting medium of the eye. Although anatomically continuous with the vascularized sclera and conjunctiva, all three major components of the cornea function together to maintain optically clear tissue. Therefore, homeostasis of the corneal epithelium, stroma, and endothelium—the cellular components of the cornea—is vital in preserving transparency and optical precision.

Stem cell researchers of the cornea have identified the epithelial stem cell to be located in the vascular rim, or limbus, of the cornea [1]. In contrast, there is little evidence of the existence of stem/progenitor cells for keratocytes [2, 3], the resident cells of the corneal stroma. Keratocytes, mesenchymal cells distinct from keratinocytes of the skin, repopulate the corneal stroma during tissue remodeling after its depletion due to disease, such as herpes simplex virus infection, and trauma [4, 5]. Although the stroma of the cornea develops from the cranial neural crest [6, 7], the origin of keratocytes involved in the turnover of stromal tissue is unknown.

We have previously demonstrated that the neurosphere culture technique, which was originally developed for neural stem cells (NSCs) isolated from the forebrain of mouse [8], can be adapted to culture mouse cornea stromal cells for more than 15 passages while still maintaining the keratocyte phenotype [9]. A recent report demonstrated that multipotent precursor cells from adult mouse and human dermis, termed skin-derived precursor cells (SKPs), also form spheres and differentiate into neural and mesenchymal cells [10–12]. We therefore hypothesized that the corneal stroma-derived spheres we have isolated also include putative keratocyte precursor cells similar to SKPs of the skin.

Correspondence: Shigeto Shimmura, M.D., Department of Ophthalmology, Keio University School of Medicine, 35 Shinanomachi, Shinjuku-ku, Tokyo 160-8582, Japan. Telephone: +81-3-3353-1211; Fax: +81-3-3359-8302; e-mail: shige@sc.itc.keio.ac.jp; or Hideyuki Okano, M.D., Ph.D., Department of Physiology, Keio University School of Medicine, 35 Shinanomachi, Shinjuku-ku, Tokyo 160-8582, Japan. Telephone: +81-3-3353-1211; Fax: +81-3-3357-5445; e-mail: hidokano@sc.itc.keio.ac.jp Received March 16, 2006; accepted for publication July 24, 2006; first published online in STEM CELLS *EXPRESS* August 3, 2006. 1066-5099/2006/$20.00/0 doi: 10.1634/stemcells.2006-0156

Table 1. Polymerase chain reaction primers

Gene		Primer sequence (5′–3′)	Product size (bp)	GenBank accession ID
Abcg2	Forward:	CCATAGCCACAGGCCAAAGT	327	NM_011920
	Reverse:	GGGCCACATGATTCTTCCAC		
Nestin	Forward:	AATGGGAGGATGGAGAATGGAC	496	NM_016701
	Reverse:	TAGACAGGCAGGGCTAAGCAAG		
Musashi1	Forward:	GGCTTCGTCACTTTCATGGACC	542	NM_008629
	Reverse:	GGGAACTGGTAGGTGTAACCAG		
Notch1	Forward:	TGCCTGTGCACACCATCCTGC	247	NM_008714
	Reverse:	CAATCAGAGATGTTGGAATGC		
Twist	Forward:	CCAGAGAAGGAGAAAATGGACAGTC	259	NM_011658
	Reverse:	AAAAAGTGGGGTGGGGGGACACAAAC		
Snail	Forward:	CCCACTCGGATGTGAAGAGATACC	534	NM_011427
	Reverse:	ATGTGTCCAGTAACCACCCTGCTG		
Slug	Forward:	CACACACACACACACACACACACAG	570	NM_011415
	Reverse:	TGTCTTTCCCTCCTCTTCCAAGG		
Sox9	Forward:	CGCCCATCACCCGCTCGCAATACG	545	NM_011448
	Reverse:	AAGCCCCTCCTCGCTGATACTGG		
Mpz	Forward:	TTCCTGCTCTCCCTTTCCTACC	422	NM_008623
	Reverse:	CCTTTCCTTCCCATTCTCGC		
Gapd	Forward:	GACCACAGTCCATGCCATCAC	453	NM_008084
	Reverse:	TCCACCACCCTGTTGCTGTAG		

Here, we show the existence of multipotent keratocyte precursor cells (termed COPs, for cornea-derived precursors) in cornea stromal spheres isolated from adult mice. Single cells dissociated from spheres initiated clonal growth of progeny spheres, and a subset of COPs exhibited the side population (SP) cell phenotype. We sought to determine whether COPs were of bone marrow (BM) origin or of neural crest lineage by initiating COP spheres in various transgenic mice.

Materials and Methods

Animals

Normal, specific pathogen-free, adult C57BL/6J mice were purchased from CLEA Japan, Inc., Tokyo, http://www.clea-japan.com/index.html). Green fluorescent protein (GFP) transgenic mice (C57BL/6 TgN [act-enhanced GFP (EGFP)] OsbC14-Y01-FM131) were obtained from the Genome Information Research Center (Osaka University, Osaka, http://www.gen-info.osaka-u.ac.jp/welcome_en.html). Transgenic mice expressing Cre recombinase under the control of the Wnt1 promoter/enhancer (Wnt1-Cre mice) [13] and P0 promoter (P0-Cre mice) [14] were mated to CAG-CAT$^{loxP/loxP}$-EGFP (CAG-CAT-EGFP) transgenic mice [15] to obtain Wnt1-Cre/CAG-CAT-EGFP (Wnt1-Cre/Floxed-EGFP) and P0-Cre/CAG-CAT-EGFP (P0-Cre/Floxed-EGFP) transgenic mice, respectively. P0-Cre transgenic mice and CAG-CAT$^{loxP/loxP}$-EGFP transgenic mice were obtained from Dr. Ken-ichi Yamamura and Dr. Jun-ichi Miyazaki, respectively. All animal procedures were performed in accordance with institutional guidelines.

Cell Culture

Cells were dissociated from adult C57BL6/J mice and then cultured as described previously [9]. All animals were handled in full accordance with the ARVO (Association for Research in Vision and Ophthalmology) Statement for the Use of Animals in Ophthalmic and Vision Research. In brief, corneal stromal discs were cut into small pieces and digested in 0.05% trypsin (Sigma-Aldrich, St. Louis, http://www.sigmaaldrich.com) for 30 minutes at 37°C, followed by 78 U/ml collagenase (Sigma-Aldrich) and 38 U/ml hyaluronidase (Sigma-Aldrich) treatment for 30 minutes at 37°C. Stromal cells were mechanically dissociated into single cells and cultured in Dulbecco's modified Eagle's medium (DMEM)/F-12 (1:1) supplemented with 20 ng/ml epidermal growth factor (EGF) (Sigma-Aldrich), 10 ng/ml fibroblastic growth factor 2 (FGF2) (Sigma-Aldrich), B27 supplement (Invitrogen, Carlsbad, CA, http://www.invitrogen.com), and 10^3 U/ml leukemia inhibitory factor (Chemicon International, Temecula, CA, http://www.chemicon.com) at a density of 1×10^5 cells per milliliter at 37°C, 5% CO_2.

For clonal sphere expansion, COPs were initiated from corneas of wild-type C57BL/6 strain and transgenic strain expressing GFP ubiquitously [16]. Cells dissociated from COPs were plated on six-well dishes at a cell density of 5×10^3 cells per milliliter and cultured for 6–7 days in DMEM/F-12 containing 0.8% methylcellulose with EGF, FGF2, and B27 supplement. The use of methyl cellulose in the clone culture of NSCs (neural spheres) is an established method reported by several groups [17–24].

To examine the expression of nestin in COPs, cells were prepared from transgenic mice carrying EGFP (Clontech, Mountain View, CA, http://www.clontech.com) under the control of the second intronic enhancer of the *nestin* gene, which acts selectively in neural stem/precursor cells (E/nestin-EGFP) [25]. To confirm the neural crest origin of COPs, corneal stromal cells were prepared from six corneas of neonatal (13 days) and three corneas of adult (8 weeks) P0-Cre/Floxed-EGFP mice, as well as from one cornea of an adult (10 weeks) Wnt1-Cre/Floxed-EGFP mouse and cultured as described above.

In Vitro Differentiation

To examine neural differentiation, COPs were dissociated into single cells and suspended at a cell density of 10 cells per milliliter. One-hundred microliters of the cell suspension was divided into 48-well culture plates, and only clonal spheres from single cells were subcultured and expanded. Clonal COPs were

plated and cultured on poly(L-ornithine)/laminin-coated Lab-Tek chamber slides (Nalge Nunc International, Rochester, NY, http://www.nalgenunc.com). For α-smooth muscle actin (α-SMA) expression, clonal cells were also plated on Lab-Tek chamber slides in transforming growth factor (TGF)-β-containing medium. For adipogenic or chondrogenic differentiation, dissociated COPs were cultured in differentiation-inducing medium (Cambrex Bio Science Walkersville, Inc., Walkersville, MD, http://www.cambrex.com) according to instructions provided by the manufacturer. To visualize adipogenic differentiation, cells were stained with oil red O (Sigma-Aldrich). Chondrogenic differentiation was observed by the expression of the specific markers collagen II and aggrecan analyzed by immunocytochemistry of cell pellets (see above). Results were expressed as mean ± SD.

Immunohistochemistry

Cultured cells and frozen-tissue sections were fixed with 4% paraformaldehyde (PFA) for 10 minutes at room temperature and then stained with the following antibodies: anti-Bcrp1 (1:250; R&D Systems, Minneapolis, http://www.rndsystems.com), anti-α-SMA (1:200; NeoMarkers, Fremont, CA, http://www.labvision.com), anti-collagen type II (1:40; Chemicon International), anti-aggrecan (1:40; Chemicon International), anti-Musashi-1 (Msi1) (1:500, clone 14H1) [26], anti-class III β-tubulin (1:100, R&D Systems), anti-glial fibrillary acidic protein (GFAP) (1:200; Chemicon International), and anti-neurofilament-M (NF-M) (1:500; Abcam, Cambridge, U.K., http://www.abcam.com). Immunohistochemistry for GFP was performed using an anti-GFP antibody (1:500; MBL, Nagoya, Japan, http://www.mbl.co.jp) in 10-μm frozen sections from eyes fixed in 2% PFA overnight at 4°C. Immunoreactivity of primary antibodies was visualized using secondary antibodies conjugated with fluorescein isothiocyanate or cyanine 3 (Jackson ImmunoResearch Laboratories, West Grove, PA, http://www.jacksonimmuno.com).

Reverse Transcription-Polymerase Chain Reaction

COPs and cells freshly dissociated from mouse corneal stroma were collected and immediately frozen in liquid N_2. cDNA was synthesized using a commercially available kit (Life Sciences, Inc., St. Petersburg, FL, http://www.lifesci.com) from total RNA prepared using RNeasy kit (Qiagen, Hilden, Germany, http://www1.qiagen.com). Primers used for *Abcg2*, *Notch1*, *nestin*, *Msi1*, *Twist*, *Snail*, *Slug*, *Sox9*, and *Gapd* are shown in Table 1 (supplemental online data). Polymerase chain reaction (PCR) was performed using GeneAmp 9700 (Applied Biosystems, Foster City, CA, http://www.appliedbiosystems.com).

Flow Cytometry

For Hoechst dye efflux assays, single cells dissociated from COP spheres were incubated with Hoechst 33342 dye (Dojindo Laboratories, Kumamoto, Japan, http://www.dojindo.com) for 60 minutes at 37°C in the presence or absence of 50 μM reserpine (Daiichi Pharmaceutical, Tokyo, http://www.daiichius.com). SP cells were gated using FACS Vantage (BD Biosciences Immunocytometry Systems, San Jose, CA, http://www.bdbiosciences.com) as described previously [27]. Surface marker expression was also analyzed by flow cytometry using antibodies for CD45, CD34, Sca-1, c-kit, and CD133 (eBioscience, San Diego, http://www.ebioscience.com). Isotype-matched immunoglobulin G was used as negative control.

BM Transplantation

Whole BM (WBM) cells (1×10^6 cells) were prepared from GFP-transgenic mice [16] and transplanted into the retro-orbital space of C57BL6/J recipient mice treated with a lethal dose (10.3 Gy) of irradiation. Eight weeks after transplantation, recipient mice were sacrificed, and corneal stromal cells were prepared for sphere culture. Cells from the transplanted animals and nonirradiated animals were then mixed and cultured as described above to assess WBM-derived cell contribution to COP sphere formation.

Results

COPs Initiate Clonal Sphere Formation

Mouse corneal stromal-derived spheres were first prepared and cultured as described previously [9]. To determine whether spheres arise from single putative COPs or from aggregates of floating cells, we first performed the clonal sphere-forming assay [17]. As shown in Figure 1, homogeneous GFP-positive or -negative spheres were found 6 days after plating. More than 70% of spheres were homogenous; however, nonclonal spheres composed of GFP-positive and -negative cells were also observed. The same observation was made by Kawase et al. [17], who reported that SKPs may aggregate at an initial cell density of 1×10^3 cells per milliliter during sphere cultures. Clonal sphere formation was observed for several passages (P5), suggesting that COPs possess high "self-renewing" potential.

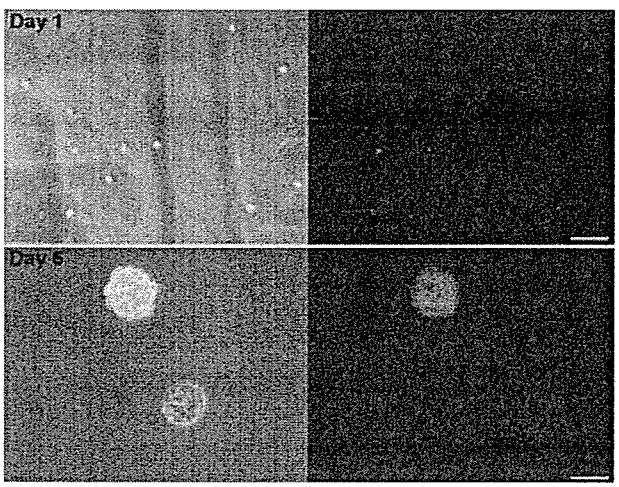

Figure 1. Single cornea-derived precursors form clonal spheres. Green fluorescent protein (GFP)-positive and -negative cells were mixed and cultured in methylcellulose-containing medium at a cell density of 5×10^3 cells per milliliter. Right and left panels show fluorescent images and phase-contrast images merged with fluorescent images, respectively. Upper panels show images of the cells 1 day after plating. After 6 days of culture, clonal spheres that consist entirely of GFP-positive or -negative cells were observed (lower panels). Scale bars = 200 μm (upper panel) and 100 μm (lower panel).